PROCEEDINGS A

royalsocietypublishing.org/journal/rspa

Research

Cite this article: De Matteis G, Giglio F, Moro A. 2024 Complete integrability and equilibrium thermodynamics of biaxial nematic systems with discrete orientational degrees of freedom. *Proc. R. Soc. A* **480**: 20230701. https://doi.org/10.1098/rspa.2023.0701

Received: 22 September 2023
Accepted: 5 January 2024

Subject Areas:
applied mathematics, mathematical physics, statistical physics

Keywords:
liquid crystals, integrability, phase transitions, biaxiality

Author for correspondence:
Francesco Giglio
e-mail: francesco.giglio@glasgow.ac.uk

Complete integrability and equilibrium thermodynamics of biaxial nematic systems with discrete orientational degrees of freedom

Giovanni De Matteis[1,2], Francesco Giglio[3] and Antonio Moro[4]

[1]Dipartimento di Matematica e Fisica, Università del Salento, Lecce, Italy
[2]I.N.F.N. Sezione di Lecce, Lecce, Italy
[3]School of Mathematics and Statistics, University of Glasgow, Glasgow, UK
[4]Department of Mathematics, Physics and Electrical Engineering, Northumbria University Newcastle, Newcastle upon Tyne, UK

FG, 0000-0003-1131-1560; AM, 0000-0002-4901-8573

We study a discrete version of a biaxial nematic liquid crystal model with external fields via an approach based on the solution of differential identities for the partition function. In the thermodynamic limit, we derive the free energy of the model and the associated closed set of equations of state involving four order parameters, proving the integrability and exact solvability of the model. The equations of state are specified via a suitable representation of the orientational order parameters, which imply two-order parameter reductions in the absence of external fields. A detailed exact analysis of the equations of state reveal a rich phase diagram where isotropic versus uniaxial versus biaxial phase transitions are explicitly described, including the existence of triple and tricritical points. Results on the discrete models are qualitatively consistent with their continuum analogue. This observation suggests that, in more general settings, discrete models may be used to capture and describe phenomena that also occur in the continuum for which exact equations of state in closed form are not available.

THE ROYAL SOCIETY PUBLISHING

1. Introduction

Mean-field models in statistical mechanics and thermodynamics are a powerful tool to explore general qualitative properties of thermodynamic systems that, otherwise, would not be analytically treatable. Both conceptual and historical importance of mean-field models is testified by the celebrated van der Waals and Curie–Weiss models [1], complemented by Maxwell's equal areas rule (e.g. [2]), which provided the first qualitative description of the mechanisms for the occurrence of phase transitions in fluids and magnetic systems. It is also well established that, in order to obtain accurate quantitative predictions, mean-field models need to be replaced by models with finite range interactions which are generally more challenging, and solvable cases require the use of sophisticated techniques as, for example, the transfer matrix and the renormalization group (e.g. [3]).

Spin models are the archetypal example of models aimed at describing the macroscopic and collective behaviour of systems made up of components with internal degrees of freedom (in the simple case the spin $\sigma = \pm 1$) with pairwise (and also higher order) interactions. Such models, although originally introduced in condensed matter physics to explain magnetic properties of materials are, however, of universal importance, as testified by applications in other disciplines such as biology, economics, social sciences (e.g. [4–6] and references therein). It is also worth noting that a resurgence of interest, in the last decade, for spin-like mean-field models is due to the studies concerning their deployment for information processing, classification, memory retrieval and, more generally, machine learning purposes [7]. These studies, originally inspired by the pioneering work of Hopfield [8], led to the definition of models for neural networks, such as the Boltzmann machines and their variations, based on spin glasses and statistical inference algorithms for training and learning [9]. The key idea in this context is that spin particles sit at a node of a graph and possess internal degrees of freedom, i.e. their spin values are interpreted as node states of the neural network associated with the graph. The spin–spin interaction constant corresponds to the weight associated with the links on the network.

In this paper, we consider a biaxial version of the discrete Maier–Saupe model for nematic liquid crystals (LCs) as studied in [10], whose structure resembles a multi-partite spin model with spin components subject to suitable constraints. The model consists of a system of particles endowed with an internal assigned geometry and symmetries with only orientational degrees of freedom. Not surprisingly, the exact analytical description of their macroscopic thermodynamic behaviour, phase transitions and emergent properties is, in general, not available and therefore alternative approaches and approximation techniques need to be adopted [11]. Numerical simulations [12], Landau's expansion of the free energy [13,14], group representation and bifurcation theory [15] are approaches that allow to explore, at least locally, i.e. in the neighbourhood of specified values for the thermodynamic parameters, the possible occurrence of criticalities and phase transitions, and estimate relevant thermodynamic quantities such as orientational order, specific heat and critical exponents. Mean-field models are effective in providing insights that complement and support the aforementioned methodologies and all together help achieve accurate qualitative description and predictions on key properties of LCs including those that are paramount for technological applications [16].

From a physical viewpoint, in the last few decades, the biaxial nematic LC phase has been the object of much intense study. The story of this phase has its roots back to 1970 [17], when the theoretical physicist Marvin Freiser noted that rather than possessing a rod-like shape (i.e. $D_{\infty h}$ symmetry), as usually assumed, most thermotropic, mesogenic molecules were in fact closer to being board-like, thus intrinsically biaxial (i.e. endowed with D_{2h} symmetry). Usually, they produce uniaxial nematic phases as a consequence of the rotational disorder around the long molecular axis, which eventually yields the definition of a single macroscopic director. This rotational disorder can be overcome by molecular mutual interactions favouring the molecules to align parallel to one another, thus leading to a thermotropic biaxial nematic phase at sufficiently

low temperatures. Accordingly, Freiser understood that mesogens should be expected to exhibit a biaxial nematic phase, in addition to the usual uniaxial one. The prediction of a second nematic phase, possessing novel properties and promising potential applications, stimulated considerable interest, as well as not little debate. In fact, on the experimental side, stable biaxial phases have been observed in lyotropic systems since the pioneering work of Yu & Saupe [18]. By contrast, the experimental proof in favour of their existence in thermotropic systems has been subject of scrutiny and criticism in [19–21]. In the period 1986–2003, the matter remained controversial with no widely accepted results [19,22,23]. However, since 2004, clearer experimental evidence was provided for a few classes of compounds, such as polar bent-core or V-shaped molecules [24–26], and organosiloxane tetrapodes or their counterparts with a germanium core [27–31]. These compounds have been investigated by several techniques which led to measurements of biaxial order parameters [32]. According to these experimental results, an alternative picture of biaxial nematic order has emerged [33–37], based on the idea of biaxial domains reoriented by surface anchoring or external fields. Other researchers [38–40] have also pointed out that the biaxial nematic order is related to the onset of smectic fluctuations. Moreover, it has also been remarked that biaxial nematics may be formed from molecules possessing a lower symmetry than the usually assumed D_{2h} one, as for instance the C_{2h} symmetry [36,41–45]. In addition, quite recently [46,47], low symmetry interaction models have been addressed, involving dipolar contribution, so as to describe polar bent-core molecules. The study of biaxial nematics is not only of theoretical origin, it is also connected with their potential technological applications in displays [33,48–52]: orientation of the secondary director in response to external perturbations is expected to be significantly faster than the primary one [34,41]. Biaxial nematic phases have also been produced in colloidal suspensions of inorganic compounds [53–55]. More recently, in [56], Smalyuhk *et al.* have considered a hybrid molecular-colloidal soft-matter system with orthorhombic biaxial orientational order and fluidity. This molecular-colloidal complex fluid is made up of only uniaxial rod-like building blocks. By contrast, this complex fluid exhibits a surprising self-assembly into a biaxial nematic LC with the D_{2h} point group symmetry. Finally, let us mention that, very recently, the emergence of biaxial order upon mechanical strain has been proved experimentally in a nematic LC elastomer, the first synthetic auxetic material at a molecular level [57]. By measuring the order parameters during deformation, the deviation from Maier–Saupe theory was detected for the uniaxial order parameters and the biaxial order parameters were deduced, suggesting the occurrence of biaxiality in the initially uniaxial system.

On the theoretical side, after Freiser's first prediction [17], investigations were actively carried out along different approaches such as molecular-field or Landau theories, and later on by computer simulations. By the end of the past century, this collection of theoretical methodologies had shown that single-component models consisting of molecules possessing D_{2h} symmetry, and interacting via various continuous or hard-core potentials, are capable of producing a biaxial nematic phase under appropriate thermodynamic conditions [33,58–60]. Theoretical studies usually predict a low-temperature biaxial phase, undergoing a transition to the uniaxial one, which, in turn, finally turns into the isotropic phase. In some cases, the transition takes place directly from the biaxial nematic to the isotropic phase. In the former cases, the ratio between the two transition temperatures (biaxial-to-uniaxial and uniaxial-to-isotropic) often turns out to be rather small in comparison with experimentally known stability ranges of the nematic phase. Both the isotropic-to-biaxial and uniaxial-to-biaxial phase transitions can be either first- or second-order, and, accordingly, the phase diagram exhibits *triple* and *tricritical points*. However, in the low-temperature range, other phases, such as smectic or solid ones, may become more likely to occur. On the other hand, most theoretical frameworks only allow for isotropic and nematic phases [34], being the positional order not accounted for. Over the years, a rather simple, continuous, biaxial mesogenic pair interaction model has been proposed and investigated by several authors and via several types of techniques. In the literature, this model is known as the *generalized Straley interaction* [61] and it finds its roots in the celebrated Maier–Saupe model for interacting uniaxial nematic molecules [62–64]. Actually, over the last two decades, several

properties of this model have emerged, such as possible simplifications, additional symmetries and versatility in applications. More precisely, in 2003, new experimental findings on biaxial nematics boosted a renewed theoretical interest by some authors [65–70]. More precisely, the generalized Straley pair potential model was studied by mean-field, as well as Monte Carlo simulation in the simple-cubic lattice-model version and, correspondingly, the effects produced on the resulting macroscopic behaviour were analysed [58,59,67,68,70,71]. Moreover, motivated by the new experimental facts, the single-tensor Landau–de Gennes theory of biaxial nematics has been carefully revisited and a double-tensor Landau theory was put forward and studied [72,73]. The hidden link between mean-field and Landau–de Gennes-type treatments has also been studied [74–76]. The Straley potential model involves three independent parameters, and the aforementioned studies have shown that the model is rather versatile and capable of producing both biaxial and purely uniaxial order. In addition, the effect of strong antinematic terms, i.e. terms promoting misalignment, in the pair potential onto the resulting orientational order has been investigated [59,77]. As shown in [77,78], these antinematic terms in the Straley model may destroy biaxiality, producing only uniaxial orientational order, and in some cases show evidence of the existence of a continuous ordering transition, in contrast with the discontinuous phase transition predicted by the simple Maier–Saupe model. Moreover, in [79], the Straley potential only contains antinematic terms, and it is found to produce biaxial order via a mechanism of order by disorder. In [61], the authors investigated the effect of two predominant antinematic couplings of equal strength perturbed by a comparatively weaker calamitic one. The resulting phases are a pure calamitic uniaxial phase, accompanied by an intermediate antinematic uniaxial phase.

In this work, we consider a *discrete* version of the celebrated Maier–Saupe model for nematic LCs as the one considered in [10] and study its *biaxial* generalization, i.e. Straley model, further extended to account for the effects of external fields. More specifically, molecules are assumed to be rigid cuboids, with two individual orientational degrees of freedom associated with two of the three principal axes of inertia, as the position of the third axis is automatically determined. It is also assumed that homologous principal axes of inertia interact pairwise for any pairs of molecules in the system. This assumption specifically characterizes the mean-field models, where indeed any pair of molecules equally interact independently of their distance, and therefore positional degrees of freedom are not relevant. A further assumption is that orientational degrees of freedom are discrete, namely principal axes can only be parallel to the directions of a predefined Cartesian reference frame. The discretization of orientational degrees of freedom for nematic LC models was firstly introduced by Zwanzig in [80] and successfully employed in various works, including recent papers [10,81]. Although this assumption may seem to be at a glance restrictive, it captures, as observed in [10], with striking accuracy, properties of the continuum model. We show, via explicit examples, that the predictions obtained under specific symmetry reductions are consistent with the ones present in the literature for the corresponding continuum models.

It is also important to note that, although, on one hand, the above assumptions restrict the model and allow to derive explicit global equations of the thermodynamic order parameters, on the other hand, the model is more general than its continuum analogues and the methodology adopted naturally incorporates external fields interacting with each orientational degree of freedom. Therefore, to the best of our knowledge, we provide the first theoretical study on the equilibrium statistical mechanics of a molecular field theory for biaxial LCs subject to external fields.

To solve the model, we show that the partition function Z_N of the N-molecules reduced Straley biaxial model with external fields satisfies a remarkable differential identity as a function of the temperature and coupling constants. Using suitably rescaled independent variables, the differential identity for the partition function of the finite size model is equivalent, up to a linear change of variables, to the heat equation. The required solution is therefore obtained by solving a linear equation with a specific initial condition that is fixed by the value of the partition function for the non-interacting model the solution of which is straightforward. The properties

royalsocietypublishing.org/journal/rspa Proc. R. Soc. A 480: 20230701

of the system in the thermodynamic regime are obtained by studying the behaviour of the free energy

$$\mathcal{F}_N := \frac{1}{N} \log Z_N$$

in the limit as $N \to \infty$, which corresponds to the *semi-classical*, or low diffusion, limit, of the heat equation, via a suitable asymptotic expansion of the free energy in powers of N^{-1}. At the leading order, the problem is solved via a Hamilton–Jacobi equation, which can be explicitly integrated, and the solution is given in terms of the orientational order parameters from which the equations of state follow as a stationary point for the free energy functional. We study in detail the solution of the Hamilton–Jacobi equation and, specifically, a related system of quasi-linear PDEs for the orientational order parameters.

The methodology based on differential identities is applied for the first time in the context of a molecular theory for biaxial nematics described by two tensor fields. We derive explicit expressions for state functions when a finite number of molecules N is considered, as well as a novel system of equations of state, which include the interaction with external fields. We rigorously classify all admissible reductions in the absence of external fields, revealing a rich singularity structure describing transitions between isotropic, uniaxial and biaxial phases. A comparison with results available in the literature shows that our findings are consistent with those obtained with different methods and techniques.

As pointed out in a number of papers [10,82–91] the nature of the PDEs derived for the orientational order parameters suggests a natural interpretation of the singularities as classical shocks propagating in the space of thermodynamic variables. This allows to explain and, qualitatively, predict some features of the phase diagram based on the general properties of shock waves, as for example the occurrence of *tricritical* points as a collision and merging mechanism of two shock waves. This example demonstrates how such an interpretation is at the same time intriguing and of practical use.

The paper is organized as follows. In §2, we introduce the physical model under study, we derive differential identities for the statistical partition function, and we provide exact solutions for the model in the finite-size regime. In §3, we perform the thermodynamic limit and derive exact equations of state for the full model. Two-parameter reductions are also obtained in the cases of (i) zero fields and (ii) non-zero fields under special constraints. In §4, we present the phase diagram of the model in the absence of external fields, and discuss criticality and behaviour of the corresponding order parameters. Section 5 is devoted to concluding remarks.

2. The discrete λ-model for biaxial nematics

Let us consider a system of N interacting LCs molecules with D_{2h} symmetry, whose molecular directors $\boldsymbol{m}$, $\boldsymbol{e}$ and $\boldsymbol{e}_\perp$ are mutually orthogonal unit vectors parallel to their principal axes. The orientational state of a given molecule is identified by the directions of its molecular axes. Introducing the tensors (e.g. [92])

$$\mathbf{q} = \boldsymbol{m} \otimes \boldsymbol{m} - \frac{1}{3}\mathbf{I} \quad \text{and} \quad \mathbf{b} = \boldsymbol{e} \otimes \boldsymbol{e} - \boldsymbol{e}_\perp \otimes \boldsymbol{e}_\perp, \tag{2.1}$$

where $\mathbf{I}$ is the 3×3 identity matrix, we consider the Hamiltonian of the form

$$H_0 = -\frac{\mu}{2N} \sum_{i,j} (\mathbf{q}_i \cdot \mathbf{q}_j + \lambda \mathbf{b}_i \cdot \mathbf{b}_j), \tag{2.2}$$

where $\mathbf{q}_i$ and $\mathbf{b}_i$ specify the orientational state of the ith molecule and the scalar product is $\mathbf{a} \cdot \mathbf{b} := \mathrm{Tr}\,(\mathbf{ab})$, where Tr is the trace operator. Summation indices i and j run from 1 to N, μ is the non-negative mean-field coupling constant and λ is a parameter weighing the degree of biaxiality. In the present paper, we assume $\lambda \in [0, 1]$. In this range, the ground state for two interacting molecules corresponds to parallel homologous axes, that is $\boldsymbol{e}_i$ tend to line up with $\boldsymbol{e}_j$, $\boldsymbol{m}_i$ with $\boldsymbol{m}_j$ and $\boldsymbol{e}_{\perp,i}$ with $\boldsymbol{e}_{\perp,j}$. When $\lambda = 0$, the above Hamiltonian reduces to the classical Maier–Saupe

model. The specific choice $\lambda = 1/3$ corresponds to the MMM model for LCs with equally nematic interaction among corresponding molecular axes [67], i.e.

$$H_1 = -\frac{\mu}{2N}\sum_{i,j}\left(\mathbf{q}_i\cdot\mathbf{q}_j + \frac{1}{3}\mathbf{b}_i\cdot\mathbf{b}_j\right)$$
$$= -\frac{\mu}{2N}\frac{2}{3}\sum_{i,j}\left[(\boldsymbol{m}_i\cdot\boldsymbol{m}_j)^2 + (\boldsymbol{e}_i\cdot\boldsymbol{e}_j)^2 + (\boldsymbol{e}_{\perp,i}\cdot\boldsymbol{e}_{\perp,j})^2 - \frac{1}{2}\right]. \tag{2.3}$$

For convenience, we have included self-interaction terms corresponding to $i = j$. This choice will not affect the result as it corresponds to a shift of the energy reference frame by a constant.

The Hamiltonian (2.2) corresponds to a Straley pair-interaction potential reduced to the case of explicit zero-coupling between $\mathbf{q}$ and $\mathbf{b}$ tensors [64,65]. Such pair-potential, identifying the so-called λ-*model*, has been studied extensively and its associated phase diagram, in the absence of external fields, has been inferred for specific two-order parameter reductions [65–67]. It is worth noticing that, although the two tensors $\mathbf{q}$ and $\mathbf{b}$ are not directly coupled in the Hamiltonian (2.2), they are geometrically related via the constraint $\mathbf{q}_i\cdot\mathbf{b}_i = 0$, thus implying an implicit microscopic coupling. As a result, the macroscopic behaviour will eventually reflect this hidden coupling through an entropic contribution in the free energy, in addition to other possible coupling terms in the order tensors, as we also show in this work.

Assuming that allowed configurations are such that molecular directors are parallel to the axes of a fixed Cartesian reference frame, the Hamiltonian (2.2) can be written as follows:

$$H_0 = -\frac{\mu}{2N}\sum_{i,j}\sum_{l,k\in\{1,2\}} c_{kl}(\Lambda_i^l\Lambda_j^k + \lambda\Lambda_i^{l+2}\Lambda_j^{k+2}),$$

where $c_{kl} = 1 + \delta_{kl}$ for $k,l = 1,2$, and Λ_i^l, with $i = 1,\dots,N$, and $l = 1,2,3,4$, parametrize the components of $\mathbf{q}_i$ and $\mathbf{b}_i$ as follows:

$$\mathbf{q}_i = \mathrm{diag}(\Lambda_i^1, \Lambda_i^2, -\Lambda_i^1 - \Lambda_i^2) \quad \text{and} \quad \mathbf{b}_i = \mathrm{diag}(\Lambda_i^3, \Lambda_i^4, -\Lambda_i^3 - \Lambda_i^4) \tag{2.4}$$

giving six possible orientational states of each molecule. In particular, we have that for the ith molecule, $\Lambda_i = (\Lambda_i^1, \Lambda_i^2, \Lambda_i^3, \Lambda_i^4) \in \{\Lambda^{(1)}, \Lambda^{(2)}, \dots, \Lambda^{(6)}\}$, where

$$\left.\begin{aligned} \Lambda^{(1)} &= \left(\frac{2}{3}, -\frac{1}{3}, 0, -1\right), & \Lambda^{(2)} &= \left(\frac{2}{3}, -\frac{1}{3}, 0, 1\right) \\ \Lambda^{(3)} &= \left(-\frac{1}{3}, \frac{2}{3}, 1, 0\right), & \Lambda^{(4)} &= \left(-\frac{1}{3}, \frac{2}{3}, -1, 0\right), \\ \Lambda^{(5)} &= \left(-\frac{1}{3}, -\frac{1}{3}, -1, 1\right) & \Lambda^{(6)} &= \left(-\frac{1}{3}, -\frac{1}{3}, 1, -1\right). \end{aligned}\right\} \tag{2.5}$$

Upon introducing the quantities $M^l = \sum_i \Lambda_i^l/N$ with $l = 1,2,3,4$, the Hamiltonian H_0 reads as follows:

$$H_0 = -\mu N[(M^1)^2 + M^1M^2 + (M^2)^2 + \lambda((M^3)^2 + M^3M^4 + (M^4)^2)]. \tag{2.6}$$

We now proceed with modelling the interaction between the LC and external fields. Consistently with previous studies on uniaxial [93–97] and biaxial nematics [10,98], we assume that the interaction between an individual biaxial liquid crystal molecule and external fields produces a term that is linear in the molecular tensors.

Let $\boldsymbol{\epsilon} = \mathrm{diag}(\epsilon_1, \epsilon_2, \epsilon_3)$ and $\boldsymbol{\chi} = \mathrm{diag}(\chi_1, \chi_2, \chi_3)$ be two tensors associated with a general external field and let H_{ex} be the Hamiltonian modelling the interaction between the external field and the LC molecules. Our assumption implies that H_{ex} is of the form

$$H_{ex} = -\sum_i (\boldsymbol{\epsilon} \cdot \mathbf{q}_i + \boldsymbol{\chi} \cdot \mathbf{b}_i) \tag{2.7}$$

$$= -N[(\epsilon_1 - \epsilon_3)M^1 + (\epsilon_2 - \epsilon_3)M^2 + (\chi_1 - \chi_3)M^3 + (\chi_2 - \chi_3)M^4]. \tag{2.8}$$

By introducing the notation $\epsilon_{k3} = \epsilon_k - \epsilon_3$ and $\chi_{k3} = \chi_k - \chi_3$ with $k = 1, 2$, we can write[1]

$$H_{ex} = -N(\epsilon_{13}M^1 + \epsilon_{23}M^2 + \chi_{13}M^3 + \chi_{23}M^4). \tag{2.9}$$

Hence, the full Hamiltonian for the mean-field model under study in this work is $H = H_0 + H_{ex}$. The associated partition function for the Gibbs distribution is given by the expression

$$Z_N = \sum_{\{(\mathbf{q},\mathbf{b})\}} \exp(-\beta H),$$

where the summation refers to all possible configurations of $(\mathbf{q}_i, \mathbf{b}_i)$ and $\beta = 1/T$ with T denoting the absolute temperature. Upon introducing the rescaled coupling constants $t := \beta\mu$, $x := \beta\epsilon_{13}$, $y := \beta\epsilon_{23}$, $z := \beta\chi_{13}$ and $w := \beta\chi_{23}$, the partition function reads as

$$Z_N = \sum_{\{(\mathbf{q},\mathbf{b})\}} \mathrm{e}^{N\{t[(M^1)^2 + M^1M^2 + (M^2)^2 + \lambda((M^3)^2 + M^3M^4 + (M^4)^2)] + xM^1 + yM^2 + zM^3 + wM^4\}}. \tag{2.10}$$

In the following, similarly to the case of van der Waals-type models [85,87], spin systems [99] and the generalization of the Maier–Saupe model in [10], we look for a differential identity satisfied by the partition function and calculate the associated initial condition. We observe that the partition function (2.10) satisfies the $(4+1)$-dimensional linear PDE

$$\frac{\partial Z_N}{\partial t} = \frac{1}{N}\left[\frac{\partial^2 Z_N}{\partial x^2} + \frac{\partial^2 Z_N}{\partial x \partial y} + \frac{\partial^2 Z_N}{\partial y^2} + \lambda\left(\frac{\partial^2 Z_N}{\partial z^2} + \frac{\partial^2 Z_N}{\partial z \partial w} + \frac{\partial^2 Z_N}{\partial w^2}\right)\right]. \tag{2.11}$$

Note that, for $\lambda > 0$, equation (2.11) can be transformed via a linear transformation of the spatial coordinates into the heat equation

$$\frac{\partial Z_N}{\partial t} = \sigma\left(\frac{\partial^2 Z_N}{\partial x'^2} + \frac{\partial^2 Z_N}{\partial y'^2} + \frac{\partial^2 Z_N}{\partial z'^2} + \frac{\partial^2 Z_N}{\partial w'^2}\right),$$

where x', y', z', w' denote the new coordinates and $\sigma = 1/N$ is the analogue of the heat conductivity. More precisely, the transformation of coordinates is given by $\mathbf{u}' = P_\lambda \mathbf{u}$, where

$$\mathbf{u}' = (x', y', z', w')^T, \quad \mathbf{u} = (x, y, z, w)^T$$

and

$$P_\lambda = \begin{pmatrix} 2 & -2 & 0 & 0 \\ 2/\sqrt{3} & 2/\sqrt{3} & 0 & 0 \\ 0 & 0 & 2/\sqrt{\lambda} & -2/\sqrt{\lambda} \\ 0 & 0 & 2/\sqrt{3\lambda} & 2/\sqrt{3\lambda} \end{pmatrix}.$$

The associated initial condition, $Z_{0,N}(x, y, z, w) := Z_N(x, y, z, w, t = 0)$, corresponds to the value of the partition function of the model for non-mutual interacting molecules. Given that the

[1]The parameters $\epsilon_{k,j}$ and $\chi_{k,j}$ can be thought of as functions of the external field applied and the properties of the material, e.g. the components of the magnetic and electric susceptibilities (e.g. [93,94,97]).

exponential is linear in the variables M^1, M^2, M^3 and M^4, the initial condition can be evaluated by recursion and gives the following formula:

$$Z_{0,N} = \left(\sum_{i=1}^{6} \mathrm{e}^{x\Lambda^{1,i} + y\Lambda^{2,i} + z\Lambda^{3,i} + w\Lambda^{4,i}} \right)^N, \tag{2.12}$$

where the index i labels the quadruples $\Lambda^{(i)} = (\Lambda^{1,i}, \Lambda^{2,i}, \Lambda^{3,i}, \Lambda^{4,i})$ defined in equations (2.5*a*) and (2.5*b*).

The exact solution to equation (2.11) for a given number of molecules N can be formally obtained by separation of variables using as a basis the set of exponential functions obtained by expanding the Nth power at the r.h.s. of equation (2.12). The solution reads as

$$Z_N = \sum_{\{\boldsymbol{k}\}} B_{\boldsymbol{k}} A_{\boldsymbol{k}}(t;\lambda) \exp(x\omega_{\boldsymbol{k}}^1 + y\omega_{\boldsymbol{k}}^2 + z\omega_{\boldsymbol{k}}^3 + w\omega_{\boldsymbol{k}}^4), \tag{2.13}$$

where $\boldsymbol{k} = (k_1, \ldots, k_6)$ is a multi-index such that $k_i = 0, \ldots, N_i$ with $N_1 = N$, $N_i = N_{i-1} - k_{i-1}$ for $i = 2, \ldots, 5$, $k_6 = N - \sum_{i=1}^{5} k_i$, $\omega_{\boldsymbol{k}}^l = \sum_{i=1}^{6} \Lambda^{l,i} k_i$, $l = 1, 2, 3, 4$ and

$$B_{\boldsymbol{k}} = \prod_{i=1}^{6} \binom{N_i}{k_i}$$

and

$$A_{\boldsymbol{k}} = \exp\left\{ \frac{t}{N} [(\omega_{\boldsymbol{k}}^1)^2 + \omega_{\boldsymbol{k}}^1 \omega_{\boldsymbol{k}}^2 + (\omega_{\boldsymbol{k}}^2)^2 + \lambda((\omega_{\boldsymbol{k}}^3)^2 + \omega_{\boldsymbol{k}}^3 \omega_{\boldsymbol{k}}^4 + (\omega_{\boldsymbol{k}}^4)^2)] \right\}.$$

Let us define the scalar order parameters m_N^1, m_N^2, m_N^3 and m_N^4 as the expectation values of, respectively, M^1, M^2, M^3 and M^4, i.e.

$$m_N^l := \langle M^l \rangle = \frac{1}{Z_N} \sum_{\{(\mathbf{q},\mathbf{b})\}} M^l \, \mathrm{e}^{-\beta H}, \quad l = 1, 2, 3, 4. \tag{2.14}$$

Upon introducing the free-energy density as $\mathcal{F}_N := (1/N) \log Z_N$, the order parameters for an intrinsically biaxial system composed by N molecules can be calculated by direct differentiation as follows:

$$m_N^1 = \frac{\partial \mathcal{F}_N}{\partial x}, \quad m_N^2 = \frac{\partial \mathcal{F}_N}{\partial y}, \quad m_N^3 = \frac{\partial \mathcal{F}_N}{\partial z} \quad \text{and} \quad m_N^4 = \frac{\partial \mathcal{F}_N}{\partial w}, \tag{2.15}$$

where $m_N^l = m_N^l(x, y, z, w, t; \lambda)$, for $l = 1, 2, 3, 4$. Equation (2.11) implies that the free-energy density satisfies the following differential identity:

$$\begin{aligned} \frac{\partial \mathcal{F}_N}{\partial t} = {} & \left(\frac{\partial \mathcal{F}_N}{\partial x} \right)^2 + \frac{\partial \mathcal{F}_N}{\partial x} \frac{\partial \mathcal{F}_N}{\partial y} + \left(\frac{\partial \mathcal{F}_N}{\partial y} \right)^2 \\ & + \lambda \left[\left(\frac{\partial \mathcal{F}_N}{\partial z} \right)^2 + \frac{\partial \mathcal{F}_N}{\partial z} \frac{\partial \mathcal{F}_N}{\partial w} + \left(\frac{\partial \mathcal{F}_N}{\partial w} \right)^2 \right] \\ & + \frac{1}{N} \left[\frac{\partial^2 \mathcal{F}_N}{\partial x^2} + \frac{\partial^2 \mathcal{F}_N}{\partial x \partial y} + \frac{\partial^2 \mathcal{F}_N}{\partial y^2} + \lambda \left(\frac{\partial^2 \mathcal{F}_N}{\partial z^2} + \frac{\partial^2 \mathcal{F}_N}{\partial z \partial w} + \frac{\partial^2 \mathcal{F}_N}{\partial w^2} \right) \right]. \end{aligned} \tag{2.16}$$

In §3, we derive the equations of state in the thermodynamic (large N) regime via a direct asymptotic approximation of the solution to equation (2.16). Before proceeding, it is worth emphasizing that the case $\lambda = 0$ implies a reduction of the model (2.16) to the one studied in [10], although the initial condition considered in that work depends on the intrinsic molecular biaxiality parameter Δ, differently from the present case in which the degree of biaxiality of the interaction is entirely contained in the internal energy term. The differences in the two treatments arise as in this paper, we are working with two order tensors, while in [10] the so-called geometric approximation on the interaction potential allowed to work with a single-order tensor, that is a linear combination of **q** and **b**.

3. Thermodynamic limit and equations of state

The thermodynamic limit is defined as the regime where the number of particles N is large, i.e. $N \to \infty$. Under the assumption that the free-energy admits the expansion of the form $\mathcal{F}_N = F + O(1/N)$ and by using equation (2.16) we obtain, at the leading order, the following Hamilton–Jacobi-type equation:

$$\frac{\partial F}{\partial t} = \left(\frac{\partial F}{\partial x}\right)^2 + \frac{\partial F}{\partial x}\frac{\partial F}{\partial y} + \left(\frac{\partial F}{\partial y}\right)^2 + \lambda\left[\left(\frac{\partial F}{\partial z}\right)^2 + \frac{\partial F}{\partial z}\frac{\partial F}{\partial w} + \left(\frac{\partial F}{\partial w}\right)^2\right]. \tag{3.1}$$

A similar asymptotic expansion for the order parameters $m^l_N = m^l + O(1/N)$ implies the relations

$$m^1 = \frac{\partial F}{\partial x}, \quad m^2 = \frac{\partial F}{\partial y}, \quad m^3 = \frac{\partial F}{\partial z} \quad \text{and} \quad m^4 = \frac{\partial F}{\partial w}.$$

Equation (3.1) is completely integrable and can be solved via the method of characteristics. In particular, the solution can be expressed via the free-energy functional

$$\begin{aligned} F = {} & xm^1 + ym^2 + zm^3 + wm^4 + t[(m^1)^2 + m^1m^2 + (m^2)^2 + \lambda((m^3)^2 + m^3m^4 + (m^4)^2)] \\ & + S(m^1, m^2, m^3, m^4), \end{aligned} \tag{3.2}$$

where m^1, m^2, m^3 and m^4 are stationary points of the free-energy, i.e:

$$\frac{\partial F}{\partial m^l} = 0 \quad \text{for } l = 1, 2, 3, 4.$$

Equivalently, order parameters are solutions to the following system of equations:

$$\left.\begin{aligned} \Psi_1 &:= x + (2m^1 + m^2)t + \frac{\partial S}{\partial m^1} = 0, \\ \Psi_2 &:= y + (m^1 + 2m^2)t + \frac{\partial S}{\partial m^2} = 0, \\ \Psi_3 &:= z + (2m^3 + m^4)\lambda t + \frac{\partial S}{\partial m^3} = 0, \\ \Psi_4 &:= w + (m^3 + 2m^4)\lambda t + \frac{\partial S}{\partial m^4} = 0. \end{aligned}\right\} \tag{3.3}$$

The term $S(m^1, m^2, m^3, m^4)$ represents the entropy of the system and, as discussed below, is uniquely fixed via the initial condition $F_0 = F(x, y, z, w, t = 0)$.

The system (3.3) represents the set of equations of state for the λ-model. Hence, phase transitions can be studied through the analysis of critical points of the equations (3.3). Similarly to the thermodynamic models studied in [85–87,90], order parameters m^l can be viewed as solutions to a nonlinear integrable system of hydrodynamic type where coupling constants x, y, z, w and t play the role of, respectively, space and time variables. In this framework, state curves within the critical region of a phase transition are the analogue of shock waves of the hydrodynamic flow. In order to specify completely equations of state (3.3), we have to determine the function $S(m^1, m^2, m^3, m^4)$. We proceed by evaluating equations (3.3) at $t = 0$, that is

$$\left.\begin{aligned} x(m^1_0, m^2_0, m^3_0, m^4_0) &= -\left.\frac{\partial S}{\partial m^1}\right|_{m^l = m^l_0}, \\ y(m^1_0, m^2_0, m^3_0, m^4_0) &= -\left.\frac{\partial S}{\partial m^2}\right|_{m^l = m^l_0}, \\ z(m^1_0, m^2_0, m^3_0, m^4_0) &= -\left.\frac{\partial S}{\partial m^3}\right|_{m^l = m^l_0}, \\ w(m^1_0, m^2_0, m^3_0, m^4_0) &= -\left.\frac{\partial S}{\partial m^4}\right|_{m^l = m^l_0}, \end{aligned}\right\} \tag{3.4}$$

where $m_0^l = m^l(x, y, z, w, t = 0)$, with $l = 1, 2, 3, 4$. Equations (3.4) show that the function $S(m^1, m^2, m^3, m^4)$ can be obtained, locally, by expressing x, y, z and w as functions of the order parameters m^l evaluated at $t = 0$ and then integrating equations (3.4). Indeed, observing that the initial condition for F is $F_0 = \mathcal{F}_{N,0} = (1/N) \log Z_{0,N}$, where $Z_{0,N}$ is given in (2.12), the required functions can be obtained by inverting the system

$$\left.\begin{aligned} m_0^1 &= \frac{\partial F_0}{\partial x}(x, y, z, w), \quad m_0^2 = \frac{\partial F_0}{\partial y}(x, y, z, w), \\ m_0^3 &= \frac{\partial F_0}{\partial z}(x, y, z, w), \quad m_0^4 = \frac{\partial F_0}{\partial w}(x, y, z, w). \end{aligned}\right\} \tag{3.5}$$

More explicitly, equations (3.5) read as follows:

$$\sum_{i=1}^{6} (m_0^l - \Lambda^{l,i}) X^{\Lambda^{1,i}} Y^{\Lambda^{2,i}} Z^{\Lambda^{3,i}} W^{\Lambda^{4,i}} = 0, \quad l = 1, 2, 3, 4, \tag{3.6}$$

where we have introduced the notation $X = \exp(x)$, $Y = \exp(y)$, $Z = \exp(z)$, $W = \exp(w)$. Hence, equations of state (3.3) for the model with external fields are completely determined in terms of the roots of system of equations (3.6). We should also emphasize that system (3.6) is algebraic with respect to the variables X, Y, Z and W.

Remark 3.1. The order parameters introduced here are related to the scalar order parameters adopted in [65] by the following linear transformation:

$$m^1 = T - \frac{S}{3}, \quad m^2 = -T - \frac{S}{3}, \quad m^3 = T' - \frac{S'}{3} \quad \text{and} \quad m^4 = -T' - \frac{S'}{3}, \tag{3.7}$$

where S, T, S', T' are the scalar order parameters characterizing the tensors $\mathbf{Q} := \langle \mathbf{q} \rangle$ and $\mathbf{B} := \langle \mathbf{b} \rangle$ in their common eigenframe, once the thermodynamic limit is performed. Specifically, by considering the eigenframe $(\boldsymbol{e}_x, \boldsymbol{e}_y, \boldsymbol{e}_z)$, the order tensors can be written as

$$\mathbf{Q} = S \left(\boldsymbol{e}_z \otimes \boldsymbol{e}_z - \frac{1}{3}\mathbf{I} \right) + T \left(\boldsymbol{e}_x \otimes \boldsymbol{e}_x - \boldsymbol{e}_y \otimes \boldsymbol{e}_y \right) \tag{3.8}$$

and

$$\mathbf{B} = S' \left(\boldsymbol{e}_z \otimes \boldsymbol{e}_z - \frac{1}{3}\mathbf{I} \right) + T' (\boldsymbol{e}_x \otimes \boldsymbol{e}_x - \boldsymbol{e}_y \otimes \boldsymbol{e}_y). \tag{3.9}$$

The inverse of the linear transformation (3.7) is

$$\left.\begin{aligned} S &= -\frac{3}{2}(m^1 + m^2), \qquad T = \frac{1}{2}(m^1 - m^2) \\ S' &= -\frac{3}{2}(m^3 + m^4), \qquad T' = \frac{1}{2}(m^3 - m^4). \end{aligned}\right\} \tag{3.10}$$

In [67], it is claimed that, in the absence of external fields, reductions $T = S' = 0$, or $T = \pm S$ and $S' = \pm 3T'$ hold, these latter obtained by swapping the axes of the reference frame, $\boldsymbol{e}_x, \boldsymbol{e}_y, \boldsymbol{e}_z$. These conditions read as $m^1 = m^2 = -S/3$ and $m^3 = -m^4 = T'$.

In the next section, we will introduce a new parametrization based on the introduction of the molecular Gibbs weights, which leads to the explicit solutions of the model.

(a) Equations of state

A convenient approach to the evaluation of the entropy of the discrete model and the corresponding equations of state starts from the statistical analysis of the 'initial condition', namely the evaluation of the partition function (2.12) as a function of the external fields at $t = 0$.

royalsocietypublishing.org/journal/rspa Proc. R. Soc. A 480: 20230701

Indeed, at $t=0$, LC molecules are mutually independent and expectation values can be evaluated by looking at the one-molecule partition function,

$$Z_{0,1}=\sum_{i=1}^{6}\mathrm{e}^{x\Lambda^{1,i}+y\Lambda^{2,i}+z\Lambda^{3,i}+w\Lambda^{4,i}}. \tag{3.11}$$

The molecular Gibbs weights [2] at $t=0$ and as functions of the external fields take the following form:

$$p_{0,i}(x,y,z,w):=\frac{\mathrm{e}^{x\Lambda^{1,i}+y\Lambda^{2,i}+z\Lambda^{3,i}+w\Lambda^{4,i}}}{Z_{0,1}},\quad i=1,\dots,6.$$

Note that the partition function (3.11), ensures that the Gibbs weights fulfil the standard normalization condition,

$$\sum_{i=1}^{6}p_{0,i}=1. \tag{3.12}$$

The configurational entropy of the model is standardly given by $S=-\sum_{k=1}^{6}p_k\log p_k$. At $t=0$, this reads, $S_0=-\sum_{k=1}^{6}p_{0,k}\log p_{0,k}$. By inspection, the following holds at $t=0$

$$\left.\begin{aligned} x&=\frac{1}{2}\log\frac{p_{0,1}p_{0,2}}{p_{0,5}p_{0,6}}, & y&=\frac{1}{2}\log\frac{p_{0,3}p_{0,4}}{p_{0,5}p_{0,6}},\\ z&=\frac{1}{2}\log\frac{p_{0,3}}{p_{0,4}}, & w&=\frac{1}{2}\log\frac{p_{0,2}}{p_{0,1}}. \end{aligned}\right\} \tag{3.13}$$

In the specific case of the model under study, one can verify that only four out of six Gibbs weights are functionally independent. Indeed, additionally to the normalization constraint (3.12), one can readily verify the following:

$$\prod_{k=1}^{3}p_{0,2k-1}=\prod_{k=1}^{3}p_{0,2k}. \tag{3.14}$$

By using equations (3.12) and (3.14), one can express $p_{0,6}$ and $p_{0,5}$ in terms of $p_{0,1}$, $p_{0,2}$, $p_{0,3}$ and $p_{0,4}$ as follows:

$$p_{0,5}=\frac{p_{0,2}p_{0,4}\left(1-\sum_{i=1}^{4}p_{0,i}\right)}{p_{0,1}p_{0,3}+p_{0,2}p_{0,4}}\quad\text{and}\quad p_{0,6}=\frac{p_{0,1}p_{0,3}\left(1-\sum_{i=1}^{4}p_{0,i}\right)}{p_{0,1}p_{0,3}+p_{0,2}p_{0,4}}. \tag{3.15}$$

Note that the entropy density, as well as the Gibbs weights, depend on the temperature and the fields via the scalar order parameters only (see equation (3.2)). Therefore, the identities in equations (3.15) hold at every t. The Gibbs weights are related to the order parameters m^l via the transformation $\varphi:(p_1,p_2,p_3,p_4)\in[0,1]^4\to(m^1,m^2,m^3,m^4)\in\mathcal{D}\subset\mathbb{R}^4$, where

$$\left.\begin{aligned} m^1&=p_1+p_2-\frac{1}{3},\\ m^2&=p_3+p_4-\frac{1}{3},\\ m^3&=\frac{(p_1p_3-p_2p_4)(1-p_1-p_2)+2p_3p_4(p_2-p1)}{p_1p_3+p_2p_4},\\ m^4&=\frac{(p_2p_4-p_1p_3)(1-p_3-p_4)+2p_1p_2(p_3-p_4)}{p_1p_3+p_2p_4}. \end{aligned}\right\} \tag{3.16}$$

The domain $\mathcal{D}$ is identified by the following constraints:

$$\frac{-2}{3}\le m^1+m^2\le\frac{1}{3},\quad -\left(\frac{2}{3}+m^1+m^2\right)\le m^1-m^2\le\frac{2}{3}+m^1+m^2$$
$$-2\le m^3-m^4\le 2,\quad -\left(\frac{2}{3}+m^1+m^2\right)\le m^3+m^4\le\frac{2}{3}+m^1+m^2.$$

Using the relations (3.13), (3.15) and (3.16), and the observation (3.4) one obtains the following set of equations for p_1, p_2, p_3 and p_4 in terms of the fields and the temperature:

$$x + (2p_1 + 2p_2 + p_3 + p_4 - 1)t - \frac{1}{2}\log\left(\frac{(p_1p_3 + p_2p_4)^2}{p_3p_4(1 - p_1 - p_2 - p_3 - p_4)^2}\right) = 0, \tag{3.17a}$$

$$y + (2p_3 + 2p_4 + p_1 + p_2 - 1)t - \frac{1}{2}\log\left(\frac{(p_1p_3 + p_2p_4)^2}{p_1p_2(1 - p_1 - p_2 - p_3 - p_4)^2}\right) = 0, \tag{3.17b}$$

$$z + \left(\frac{p_1p_3(1 - 2p_1 + p_3 - 3p_4 - p_2p_4(1 - 2p_2 - 3p_3 + p_4))}{p_1p_3 + p_2p_4}\right)\lambda t - \frac{1}{2}\log\left(\frac{p_3}{p_4}\right) = 0, \tag{3.17c}$$

$$w + \left(\frac{p_2p_4(1 - 3p_1 + p_2 - 2p_4) - p_1p_3(1 + p_1 - 3p_2 - 2p_3)}{p_1p_3 + p_2p_4}\right)\lambda t - \frac{1}{2}\log\left(\frac{p_2}{p_1}\right) = 0. \tag{3.17d}$$

Equations (3.17*a*)–(3.17*d*) can be viewed as the equations of state of the discrete λ-model subject to external fields, parametrized by p_i and intensive thermodynamic variables x, y, z, w and t, which are the control parameters of the model. Note that equations (3.17*a*)–(3.17*d*) are the critical points of the free-energy which can now be given the form

$$F = x\,m^1 + y\,m^2 + z\,m^3 + w\,m^4 + \frac{t}{2}[\mathrm{Tr}\,\mathbf{Q}^2 + \lambda\,\mathrm{Tr}\,\mathbf{B}^2] - \sum_{k=1}^{6} p_k \log p_k, \tag{3.18}$$

where $\mathbf{Q} = \mathrm{diag}(m^1, m^2, -m^1 - m^2)$ and $\mathbf{B} = \mathrm{diag}(m^3, m^4, -m^3 - m^4)$, and $m^l = m^l(p_1, p_2, p_3, p_4)$, with $l = 1, 2, 3, 4$, and $p_{5,6} = p_{5,6}(p_1, p_2, p_3, p_4)$ are given by equations (3.16) and (3.15), respectively.

(i) Two-parameter reductions

In this subsection, we will focus on the derivation of two-parameter reductions of the equations of state (3.17*a*)–(3.17*d*). Such reductions arise naturally when considering the LC system constrained to suitable forms of external fields, including the case in which external fields are not present and the phase behaviour is entirely regulated by the mutual interactions among LC molecules and the temperature. The following holds in the absence of external fields.

Lemma 3.2. *In the absence of external fields, that is at $x = y = z = w = 0$, solutions to the system (3.17a)–(3.17d) are given by one of the following two-parameter reductions:*

(i) (a) $p_4 = p_2$ and $p_3 = p_1$, with

$$(1 - 3p_1 - 3p_2)t = \frac{1}{2}\log\left(\frac{p_1p_2(1 - 2p_1 - 2p_2)^2}{(p_1^2 + p_2^2)^2}\right) \tag{3.19}$$

and

$$(p_1 - p_2)\left(1 + \frac{4p_1p_2 - p_1 - p_2}{p_1^2 + p_2^2}\right)\lambda t = \frac{1}{2}\log\left(\frac{p_2}{p_1}\right). \tag{3.20}$$

(b) $p_3 = [(1 - 2p_1 - 2p_2)p_2^2]/(p_1^2 + p_2^2)$ and $p_4 = [(1 - 2p_1 - 2p_2)p_1^2]/(p_1^2 + p_2^2)$, where p_1 and p_2 satisfy equations (3.19)–(3.20).

(c) $p_1 = [(1-2p_3-2p_4)p_4^2]/(p_3^2+p_4^2)$ *and* $p_2 = [(1-2p_3-2p_4)p_3^2]/(p_3^2+p_4^2)$, *where* p_3 *and* p_4 *satisfy*

$$(1-3p_3-3p_4)t = \frac{1}{2}\log\left(\frac{p_3p_4(1-2p_3-2p_4)^2}{(p_3^2+p_4^2)^2}\right) \tag{3.21}$$

and

$$(p_4-p_3)\left(1+\frac{4p_3p_4-p_3-p_4}{p_3^2+p_4^2}\right)\lambda t = \frac{1}{2}\log\left(\frac{p_3}{p_4}\right). \tag{3.22}$$

(ii) (a) $p_3 = p_2$ *and* $p_4 = p_1$, *with*

$$(1-3p_1-3p_2)t = \frac{1}{2}\log\left(\frac{(1-2p_1-2p_2)^2}{4p_1p_2}\right) \tag{3.23}$$

and

$$3(p_1-p_2)\lambda t = \frac{1}{2}\log\left(\frac{p_1}{p_2}\right). \tag{3.24}$$

(b) $p_3 = p_4 = 1/2 - p_1 - p_2$, *with equations (3.23) and (3.24) holding for* p_1 *and* p_2.

(c) $p_2 = p_1 = 1/2 - p_3 - p_4$, *with*

$$(1-3p_3-3p_4)t = \frac{1}{2}\log\left(\frac{(1-2p_3-2p_4)^2}{4p_3p_4}\right) \tag{3.25}$$

and

$$3(p_4-p_3)\lambda t = \frac{1}{2}\log\left(\frac{p_4}{p_3}\right). \tag{3.26}$$

Proof. Let us consider equations (3.17*a*)–(3.17*d*) restricted to the condition $x = y = z = w = 0$. Observing that equation (3.17*a*) has special solutions such that

$$2p_1 + 2p_2 + p_3 + p_4 - 1 = 0 \tag{3.27}$$

and

$$(p_1p_3 + p_2p_4)^2 - p_3p_4(1-p_1-p_2-p_3-p_4)^2 = 0, \tag{3.28}$$

the above system admits two solutions for p_3 and p_4 as functions of p_1 and p_2: one is $p_3 = [(1-2p_1-2p_2)p_2^2]/(p_1^2+p_2^2)$, $p_4 = [(1-2p_1-2p_2)p_1^2]/(p_1^2+p_2^2)$, and the other is $p_3 = p_4 = 1/2 - p_1 - p_2$. Substituting the first into equation (3.17*b*), we obtain equation (3.19), while the same constraints imply that equations (3.17*c*)–(3.17*d*) reduce to equation (3.19), thus proving reduction (i) (b). If we consider the second solution instead, we obtain (3.23) from equations (3.17*b*) and (3.24) from equations (3.17*c*) and (3.17*d*), thus proving reduction (ii) (b). Similarly, equation (3.17*b*) admits solutions such that

$$2p_3 + 2p_4 + p_1 + p_2 - 1 = 0 \tag{3.29}$$

and

$$(p_1p_3 + p_2p_4)^2 - p_1p_2(1-p_1-p_2-p_3-p_4)^2 = 0, \tag{3.30}$$

which provide two solutions: one is $p_1 = [(1-2p_3-2p_4)p_4^2]/(p_3^2+p_4^2)$, $p_2 = [(1-2p_3-2p_4)p_3^2](p_3^2 + p_4^2)$, and the other is $p_2 = p_1$ and $p_3 = 1/2 - p_1 - p_4$. Substituting the first solution into equation (3.17*a*), one obtains (3.44), while the same constraints imply that equations (3.17*c*) and (3.17*d*) reduce to equation (3.25), that is the reduction (i) (c). If we consider the second solution instead, we obtain (3.23) from equation (3.17*b*) and (3.24) from equation (3.17*c*) and (3.17*d*), thus

yielding reduction (ii) (c). When $2p_1+2p_2+p_3+p_4-1\neq 0$ and $2p_3+2p_4+p_1+p_2-1\neq 0$, we can eliminate t from equations (3.17*a*)–(3.17*b*) to get the following:

$$\log\left(\frac{p_1p_3+p_2p_4}{p_3p_4}\right)=\frac{p_1+p_2-p_3-p_4}{1-p_1-p_2-2p_3-2p_4}\log\left(\frac{(1-p_1-p_2-p_3-p_4)^2}{p_1p_3+p_2p_4}\right)+\frac{1-2p_1-2p_2-p_3-p_4}{1-p_1-p_2-2p_3-2p_4}\log\left(\frac{p_1p_3+p_2p_4}{p_1p_2}\right). \tag{3.31}$$

Let $k>0$ be an arbitrary constant and ϑ be the scale transformation defined by $\vartheta: p_i\to kp_i$ for $i=1,2,4,6$. The l.h.s. of equation (3.31) is invariant under the action of ϑ, and is therefore independent of k. For consistency, the r.h.s. must retain the same property. By applying ϑ to equation (3.31) and requiring that the r.h.s. is does not dependent on k, one obtains that solutions satisfy

$$p_1+p_2=p_3+p_4. \tag{3.32}$$

We proceed by eliminating the factor λt from equations (3.17*c*) and (3.17*d*), obtaining

$$\log\left(\frac{p_1}{p_2}\right)=\frac{(1-3p_1+p_2-2p_4)p_2p_4-(1+p_1-2p_3-3p_2)p_1p_3}{(1-2p_1+p_3-3p_4)p_1p_3-(1-2p_2-3p_3+p_4)p_2p_4}\times\log\left(\frac{p_3}{p_4}\right). \tag{3.33}$$

The generic solution is obtained by the same scaling argument. More precisely, invariance of both sides of equation (3.33) under the action of ϑ gives $(p_1p_3-p_2p_4)(p_1p_3+p_2p_4)(p_1+p_4-p_2-p_3)\log(p_4/p_3)=0$, which can be realized in the two following cases:

$$p_1+p_4=p_2+p_3 \tag{3.34}$$

and

$$p_1p_3=p_2p_4. \tag{3.35}$$

System of equations (3.32)–(3.34) has solutions $p_3=p_1$ and $p_4=p_2$, while system of equations (3.32)–(3.35) has solutions $p_3=p_2$ and $p_4=p_1$. By imposing the first of the two sets of constraints to equations (3.17*a*)–(3.17*d*), one obtains the system of equations (3.19) and (3.20), hence proving the reduction (i) (a), while the second set of constraints gives equations (3.23) and (3.24), thus proving the reduction (ii) (a). ■

As we prove in theorem 3.3, lemma 3.1 has a remarkable implication on the structure of the two order tensors of the theory. In order to proceed, it may be convenient to recall a criterion to characterize the degree of biaxiality of a given order tensor $\boldsymbol{\Omega}$. This will be based on the *biaxiality parameter* $\beta^2(\boldsymbol{\Omega}):=1-6(\mathrm{Tr}^2(\boldsymbol{\Omega}^3)/\mathrm{Tr}^3(\boldsymbol{\Omega}^2))$, satisfying $0\leq\beta^2\leq 1$ [100].

Definition 3.3. A tensor $\boldsymbol{\Omega}$ is said to be uniaxial if $\beta^2(\boldsymbol{\Omega})=0$ and biaxial if $0<\beta^2(\boldsymbol{\Omega})\leq 1$. Furthermore, in the extreme case $\beta^2(\boldsymbol{\Omega})=1$, $\boldsymbol{\Omega}$ is said to be maximally biaxial.

The following theorem characterizes the allowed forms of the two order tensors of the model.

Theorem 3.4. *In the absence of external fields, at all temperatures and values of* λ*, the order tensors take one of the following two forms*

(*i*) **Q** *uniaxial and* **B** *maximally biaxial;*
(*ii*) **Q** *and* **B** *both uniaxial.*

Proof. The result is readily obtained by considering lemma 3.1 and the transformation φ specified by equations (3.16). The subcases (a), (b) and (c) of lemma 3.1 in each of the two cases (i)

and (ii), correspond to a particular choice of the principal axis. For instance, the transformation φ evaluated along with case (i) (a) implies $\mathbf{Q} = \mathrm{diag}\,(m^1, m^1, -2\,m^1)$ and $\mathbf{B} = \mathrm{diag}\,(m^3, -m^3, 0)$, with

$$m^2 = m^1 = -\frac{1}{3} + p_1 + p_2$$

and

$$m^4 = -m^3 = (p_1 - p_2)\left(1 + \frac{4p_1p_2 - p_1 - p_2}{p_1^2 + p_2^2}\right),$$

while case (ii) (a) leads to $\mathbf{Q} = \mathrm{diag}\,(m^1, m^1, -2m^1)$ and $\mathbf{B} = \mathrm{diag}\,(m^3, m^3, -2m^3)$, with

$$m^2 = m^1 = -\frac{1}{3} + p_1 + p_2 \quad \text{and} \quad m^4 = m^3 = p_2 - p_1.$$

Similarly, case (i) (b) corresponds to $\mathbf{Q} = \mathrm{diag}\,(m^1, -2m^1, m^1)$ and $\mathbf{B} = \mathrm{diag}\,(m^3, 0, -m^3)$, with

$$m^2 = -2m^1 = 2\left(\frac{1}{3} - p_1 - p_2\right)$$

and

$$m^3 = (p_1 - p_2)\left(1 + \frac{4p_1p_2 - p_1 - p_2}{p_1^2 + p_2^2}\right), \quad m^4 = 0,$$

and case (ii) (b) corresponds to $\mathbf{Q} = \mathrm{diag}\,(m^1, -2m^1, m^1)$ and $\mathbf{B} = \mathrm{diag}\,(m^3, -2m^3, m^3)$, with

$$m^2 = -2m^1 = 2\left(\frac{1}{3} - p_1 - p_2\right) \quad \text{and} \quad m^4 = -2m^3 = -2(p_1 - p_2).$$

Finally, case (i) (c) corresponds to $\mathbf{Q} = \mathrm{diag}\,(-2m^2, m^2, m^2)$ and $\mathbf{B} = \mathrm{diag}\,(0, m^4, -m^4)$, with

$$m^1 = -2m^2 = 2\left(\frac{1}{3} - p_3 - p_4\right)$$

and

$$m^3 = 0, m^4 = (p_4 - p_3)\left(1 + \frac{4p_3p_4 - p_3 - p_4}{p_3^2 + p_4^2}\right),$$

and case (ii) (c) leads to $\mathbf{Q} = \mathrm{diag}\,(-2m^2, m^2, m^2)$ and $\mathbf{B} = \mathrm{diag}\,(-2m^4, m^4, m^4)$, with

$$m^2 = m^1 = -\frac{1}{3} + p_1 + p_2 \quad \text{and} \quad m^3 = -2m^4 = 1 - 2p_1 - 4p_4.$$

The statement is proven by evaluating the biaxiality parameter β^2 for $\mathbf{Q}$ and $\mathbf{B}$ along all cases. Due to the invariance by exchange of principal axes, β^2 for $\mathbf{Q}$ and $\mathbf{B}$ will take same values for all subcases (a), (b) and (c) of a given case. Without loss of generality, we can consider cases (i) (a) and (ii) (a) to get, respectively,

(i) $\beta^2(\mathbf{Q}) = 1 - 6(\mathrm{Tr}^2(\mathrm{diag}\,((m^1)^3, (m^1)^3, -8(m^1)^3))/\mathrm{Tr}^3)(\mathrm{diag}\,((m^1)^2, (m^1)^2, 4(m^1)^2)) = 0$,
$\beta^2(\mathbf{B}) = 1 - 6(\mathrm{Tr}^2(\mathrm{diag}((m^3)^3, -(m^3)^3, 0))/\mathrm{Tr}^3(\mathrm{diag}((m^3)^2, (m^3)^2, 0))) = 1$, that is $\mathbf{Q}$ uniaxial and $\mathbf{B}$ maximally biaxial;

(ii) $\beta^2(\mathbf{Q}) = 1 - 6(\mathrm{Tr}^2(\mathrm{diag}\,((m^1)^3, (m^1)^3, -8(m^1)^3))/\mathrm{Tr}^3(\mathrm{diag}\,((m^1)^2, (m^1)^2, 4(m^1)^2))) = 0$,
$\beta^2(\mathbf{B}) = 1 - 6(\mathrm{Tr}^2(\mathrm{diag}((m^3)^3, (m^3)^3, -8(m^3)^3))/\mathrm{Tr}^3(\mathrm{diag}((m^3)^2, (m^3)^2, 4(m^3)^2))) = 0$, hence $\mathbf{Q}$ and $\mathbf{B}$ both uniaxial.

■

A direct consequence of the reductions (ii) in theorem 3.3 and the transformation φ is the following corollary.

Corollary 3.5. *The equations of state for the model in the case of* $\mathbf{Q}$ *and* $\mathbf{B}$ *both uniaxial, cases (ii) in Theorem (3.3), can be written explicitly in terms of the eigenvalues* m^I. *In particular, we have that reductions (ii) (a), (b) and (c) can be written as follows:*

(*ii*) (*a*) $m^2 = m^1$ *and* $m^4 = m^3$ *with*

$$6m^1 t = \log\left(\frac{(1+3m^1+3m^3)(1+3m^1-3m^3)}{(1-6m^1)^2}\right) \tag{3.36}$$

and

$$6m^3\lambda t = \log\left(\frac{1+3m^1+3m^3}{1+3m^1-3m^3}\right); \tag{3.37}$$

(*b*) $m^2 = -2m^1$ *and* $m^4 = -2m^3$ *with* m^1 *and* m^3 *specified by equations (3.36) and (3.37);*
(*c*) $m^1 = -2m^2$ *and* $m^3 = -2m^3$ *with*

$$6m^2 t = \log\left(\frac{(1+3m^2+3m^4)(1+3m^2-3m^4)}{(1-6m^2)^2}\right) \tag{3.38}$$

and

$$6m^4\lambda t = \log\left(\frac{1+3m^2+3m^4}{1+3m^2-3m^4}\right). \tag{3.39}$$

Proof. As shown in the proof of Theorem (3.3), the transformation φ is linear when restricted to the case of **Q** and **B** both uniaxial. Hence, the transformation can be easily inverted to get the projection $\varphi^{-1}:(m^1,m^2,m^3,m^4)\longmapsto(p_1,p_2,p_3,p_4)$ along with each particular two-parameter reduction. The equations in terms of the eigenvalues are then obtained by application of the inverse transformation for the specific reduction to the corresponding set of equations in the p-variables. Taking the case (ii) (a) as an example, the application of $\varphi_a^{-1} := \{\varphi|_{p_3=p_2,p_4=p_1}\}^{-1}$ explicitly given by

$$\varphi_a^{-1}:(m^1,m^3)\longmapsto(p_1,p_2)=\left(\frac{1+3m^1-3m^3}{6},\frac{1+3m^1+3m^3}{6}\right),$$

to equations (3.23) and (3.24) gives equations (3.36) and (3.37). Equations (3.36) and (3.37) and (3.38) and (3.39) for (b) and (c), respectively, are obtained in a similar fashion. ∎

Unlike uniaxial–uniaxial reductions discussed above, uniaxial–maximally biaxial reductions cannot be written in explicit simple form in terms of the m^l variables.

In this paper, we will focus our discussion on the phase behaviour in the absence of external fields. We note, however, that the above reductions are also compatible with non-zero fields values subject to suitable constraints. Indeed, the following proposition allows to identify the constraints on the external fields so that the system admits *uniaxial–maximally biaxial* and *uniaxial–uniaxial* solutions for **Q** and **B**. In such cases, we can still consider two-parameter reductions of the system, with the equations of state also accounting for the action of applied fields.

Proposition 3.6. *In the presence of external fields, the system (3.17a)–(3.17d) admits the following uniaxial–maximally biaxial two-parameter reductions:*

(*i*) (*a*) $p_3 = p_1$ *and* $p_4 = p_2$, *provided that external fields satisfy* $y = x$ *and* $w = -z$, *that is* $\epsilon_1 = \epsilon_2$ *and* $\chi_3 = (\chi_1+\chi_2)/2$, *specified by*

$$x + (3p_1+3p_2-1)t = \frac{1}{2}\log\left(\frac{(p_1^2+p_2^2)^2}{p_1p_2(1-2p_1-2p_2)^2}\right) \tag{3.40}$$

and

$$z + (p_2-p_1)\left(1+\frac{4p_1p_2-p_1-p_2}{p_1^2+p_2^2}\right)\lambda t = \frac{1}{2}\log\left(\frac{p_1}{p_2}\right) \tag{3.41}$$

(*b*) $p_3 = ((1-2p_1-2p_2)p_2^2/(p_1^2+p_2^2))$ *and* $p_4 = (1-2p_1-2p_2)p_1^2/(p_1^2+p_2^2)$, *provided that* $x=0$ *and* $z=2w$, *that is* $\epsilon_1=\epsilon_3$ *and* $\chi_2=(\chi_1+\chi_3)/2$, *specified by*

$$y+(1-3p_1-3p_2)t=\frac{1}{2}\log\left(\frac{p_1p_2(1-2p_1-2p_2)^2}{(p_1^2+p_2^2)^2}\right) \tag{3.42}$$

and

$$w+(p_1-p_2)\left(1+\frac{4p_1p_2-p_1-p_2}{p_1^2+p_2^2}\right)\lambda t=\frac{1}{2}\log\left(\frac{p_2}{p_1}\right) \tag{3.43}$$

(*c*) $p_1 = (1-2p_3-2p_4)p_4^2/(p_3^2+p_4^2)$ *and* $p_2 = (1-2p_3-2p_4)p_3^2/(p_3^2+p_4^2)$, *provided that* $y=0$ *and* $w=2z$, *that is* $\epsilon_2=\epsilon_3$ *and* $\chi_1=(\chi_2+\chi_3)/2$, *and specified by*

$$x+(1-3p_3-3p_4)t=\frac{1}{2}\log\left(\frac{p_3p_4(1-2p_3-2p_4)^2}{(p_3^2+p_4^2)^2}\right) \tag{3.44}$$

and

$$z+(p_4-p_3)\left(1+\frac{4p_3p_4-p_3-p_4}{p_3^2+p_4^2}\right)\lambda t=\frac{1}{2}\log\left(\frac{p_3}{p_4}\right) \tag{3.45}$$

and uniaxial–uniaxial two-parameter reductions:

(*ii*) (*a*) $p_3=p_2$ *and* $p_4=p_1$, *provided that* $x=y$ *and* $z=w$, *that is* $\epsilon_1=\epsilon_2$ *and* $\chi_1=\chi_2$, *specified by*

$$x+(3p_1+3p_2-1)t=\frac{1}{2}\log\left(\frac{4p_1p_2}{(1-2p_1-2p_2)^2}\right) \tag{3.46}$$

and

$$z+3(p_2-p_1)\lambda t=\frac{1}{2}\log\left(\frac{p_2}{p_1}\right) \tag{3.47}$$

(*b*) $p_3=p_4=\frac{1}{2}-p_1-p_2$, *provided by* $x=0$ *and* $z=0$, *that is* $\epsilon_1=\epsilon_3$ *and* $\chi_1=\chi_3$, *specified by*

$$y+(1-3p_1-3p_2)t=\frac{1}{2}\log\left(\frac{(1-2p_1-2p_2)^2}{4p_1p_2}\right) \tag{3.48}$$

and

$$w+3(p_2-p_1)\lambda t=\frac{1}{2}\log\left(\frac{p_2}{p_1}\right) \tag{3.49}$$

(*c*) $p_2=p_1=\frac{1}{2}-p_3-p_4$, *provided that* $y=0$ *and* $w=0$, *that is* $\epsilon_2=\epsilon_3$ *and* $\chi_2=\chi_3$, *specified by*

$$x+(1-3p_3-3p_4)t=\frac{1}{2}\log\left(\frac{(1-2p_3-2p_4)^2}{4p_3p_4}\right) \tag{3.50}$$

and

$$z+3(p_3-p_4)\lambda t=\frac{1}{2}\log\left(\frac{p_3}{p_4}\right). \tag{3.51}$$

Proof. The constraints on the fields follow from looking for either uniaxial–maximally biaxial or uniaxial–uniaxial reductions of the whole set of equations of state, equations (3.17*a*)–(3.17*d*). For instance, the uniaxial–maximally biaxial reduction (i) (a) requires $p_3=p_1$ and $p_4=p_2$. Equations (3.17*a*)–(3.17*d*) restricted to this constraint imply that compatibility of the first two equations restricts fields to $y=x$, while compatibility of the third and fourth requires $w=-z$. Elementary algebraic manipulations lead to equations (3.40) and (3.41). The set of field-dependent equations of state in the case (i) (b) and (c), and (ii) (a), (b) and (c) are obtained following the same procedure, together with the associated constraints on the fields. ∎

4. Order parameters in the two-parameter reductions

The equations of state (3.17*a*)–(3.17*d*) are the critical points of the free-energy functional (3.18). According to the definition of free-energy adopted in this paper, global maxima identify stable states of the system and associated phases. Coexistence curves (hypersurfaces, in general) arise as sets of control parameters for which two or more local maxima are resonant, hence identifying the coexistence of the corresponding phases. In order to proceed, we should therefore first identify all local maxima for each choice of control parameters x, y, z, w, λ and t. In this section, we focus on the complete characterization of the system in the absence of external fields, i.e. $x = y = z = w = 0$, hence relying on theorem 3.3 and its implications. An immediate consequence is that the onset of phase transitions is determined by analysing the singularities of two-dimensional maps defined by equations (3.19) and (3.26) (see [10] for an exhaustive treatment). Noticeably, this is a more affordable task compared with the full four-dimensional problem governing the system when external fields are present, equations (3.17*a*)–(3.17*d*).

By evaluating the Hessian matrix of the free energy density (3.18), it turns out that none of the critical points in the uniaxial–uniaxial reductions, cases (ii) (a–c) in lemma 3.1) are stable. This result is consistent with what is known from mean-field theories based on a continuum of molecular orientational states [67]. Therefore, the uniaxial–maximally biaxial reductions, cases (i) (a)–(c) in lemma 3.1, are the only ones relevant from the equilibrium thermodynamics viewpoint. The following subsections focus on the analysis of the resulting phase diagram and the associated order parameters' behaviour, with case (i) (a) being considered for such purpose. Cases (i) (b) and (i) (c) can be straightforwardly obtained from case (i) (a) via suitable linear transformations on m^1 and m^3, which merely correspond to permutations of axes.

(a) Phase behaviour in the absence of external fields

The phase diagram of the model in the absence of external fields is shown in figure 1. The top row shows the phase diagram in the $\lambda - t$ plane, while the bottom row shows the phase diagram in the $\lambda - T^*$ plane, where T^* is the dimensionless temperature defined by $T^* := 1/t = (k_B T)/\mu$. The λ–t plane is divided in three regions identifying three distinct macroscopic phases, namely the *isotropic* (*I*), the *uniaxial nematic* (*U*) and the *biaxial nematic* (*B*). The lines separating the different regions are either dotted black lines or solid black lines. The former identify the so-called second-order transition lines, that is the lines associated with phase changes characterized by continuous order parameters but discontinuous derivatives. The latter are instead associated with first-order lines, that is the order parameters and their derivatives experience a discontinuity when the line is crossed. Similarly to the analysis performed in [10], second-order lines are identified by cusp points of two-dimensional maps. The cusp points of the model (red lines in figure 1) are given explicitly in terms of the transcendental curve

$$\mathcal{C} = \left\{ (\lambda, t) \in [0,1] \times [0, +\infty) \,|\, \mathrm{e}^{t-(1/\lambda)}(2 - \lambda t) + 1 - 2\lambda t = 0 \right\}.$$

Note that the cusp set can be seen as the union of two curves intersecting at the point $(\lambda, t) = (1/3, 3)$. The model admits two tricritical points, $(\lambda_{\mathrm{tc}}^{(UB)}, t_{\mathrm{tc}}^{(UB)}) = (0.217, 2.854)$ (red circle) and $(\lambda_{\mathrm{tc}}^{(IB)}, t_{\mathrm{tc}}^{(IB)}) = (2/3, 3/2)$ (blue circle). The three phases coexist at the triple point, $(\lambda_{\mathrm{tp}}, t_{\mathrm{tp}}) = (0.234, 2.773)$ (green circle) identified by the resonance condition for the corresponding maxima. A closer look in the region surrounding the triple point and the uniaxial–biaxial tricritical point is provided in the right column. The cusp points in the $\lambda - T^*$ plane are given by the set

$$\mathcal{C}^* = \left\{ (\lambda, T^*) \in [0,1]^2 \,|\, \mathrm{e}^{(1/T^*)-(1/\lambda)} \left(2 - \frac{\lambda}{T^*}\right) + 1 - \frac{2\lambda}{T^*} = 0 \right\}.$$

The constraint $\lambda = T^*$ identifies the subset of cusp points associated with second-order lines for $\lambda \geq 2/3$.

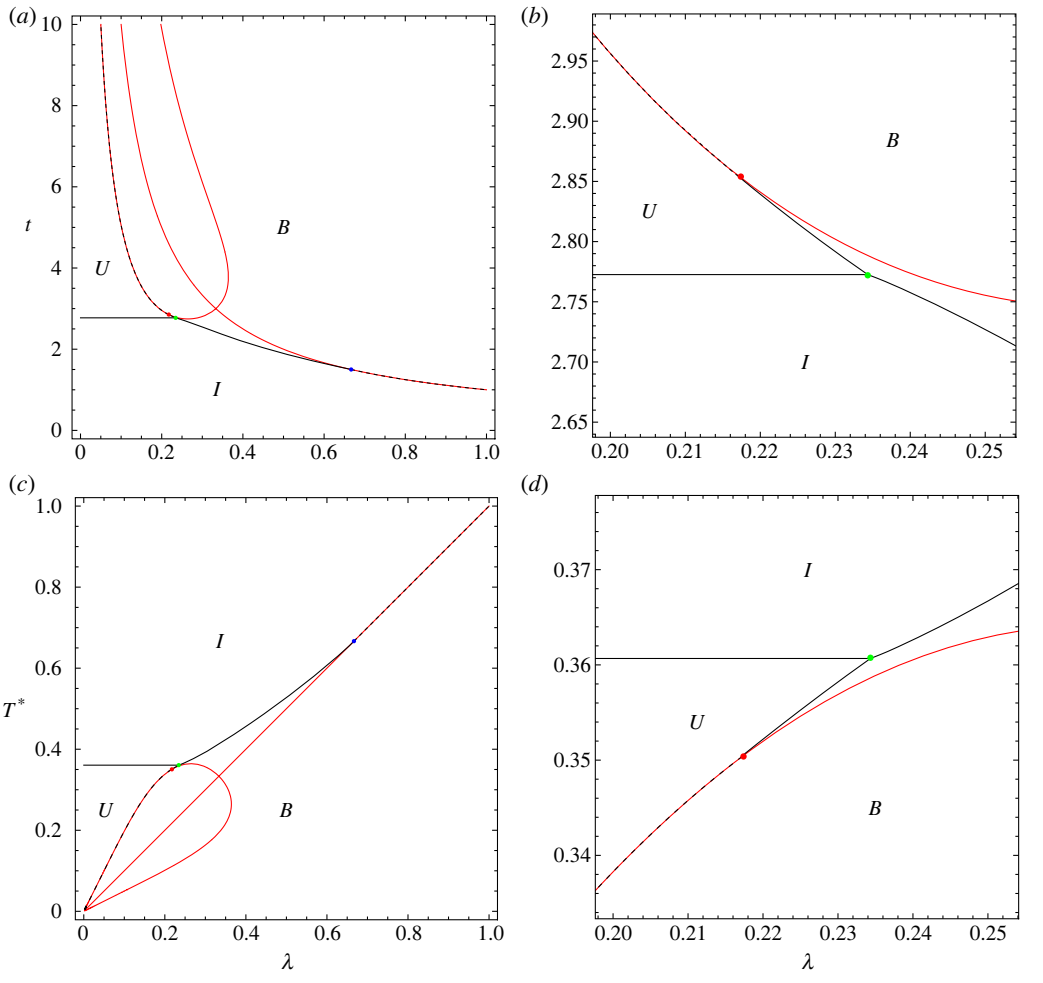

Figure 1. Zero-fields phase diagram. (*a*,*b*) phase diagram in the $\lambda - t$ plane. (*c*,*d*) phase diagram in the $\lambda - T^*$ plane. The figures in (*b*,*d*) represent a magnification of the phase diagram in the region surrounding the triple point (green circle) and the uniaxial–biaxial tricritical point (red circle). The line associated with uniaxial cusp points is indicated in red.

(b) Order parameters in the absence of external fields

In this section, we analyse the order parameters' behaviour for the reduction $m^2 = m^1$, $m^4 = -m^3$ in the absence of external fields as the temperature changes. Following our discussion on the phase diagram displayed in figure 1, we proceed by showing the expectation values m^1 and m^3 at different increasing values of λ. The values chosen for λ aim at displaying the whole phenomenology predicted by the phase diagram.

Figure 2 shows the behaviour of order parameters in the absence of external fields for small values of λ. The case $\lambda = 0$ (*a*,*d*) reproduces the phenomenology of the standard Maier–Saupe model, with the biaxial order parameter vanishing and a discontinuous isotropic-to-uniaxial nematic phase transition at $t_c^{NI} = 4 \log 2$. For small values of λ (*b*,*e*), that is $0 < \lambda < \lambda_{tc}^{UB} \approx 0.217$, additionally to the isotropic-to-nematic phase transition, a continuous phase change at lower temperatures is displayed from the uniaxial phase to the biaxial phase. Consistently with the phase diagram in figure 1, the uniaxial-to-biaxial phase transition becomes first-order at the uniaxial-biaxial tricritical point (*c*,*f*), where both order parameters experience a gradient catastrophe at $t = t_{tc}^{(UB)} = 2.854$.

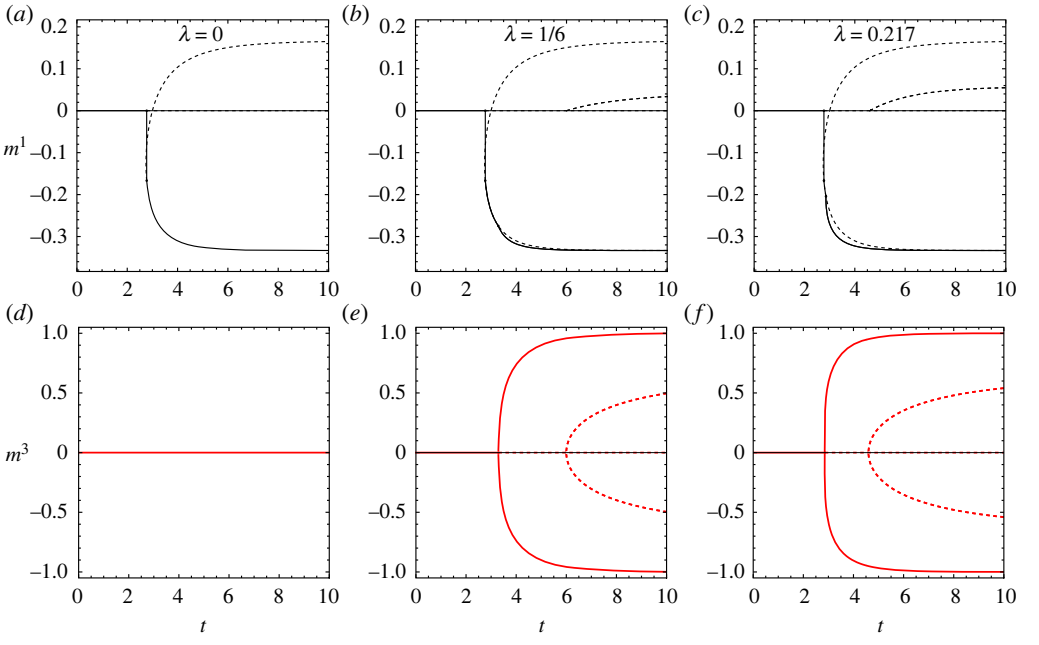

Figure 2. Order parameters in the two-parameter reduction for small values of λ. Each column shows both order parameters, m^1 (black) and m^3 (red) versus t at a specific value of λ. The solutions corresponding to a global maximum of the free energy are displayed with solid lines, while other solutions are indicated with dotted lines. (*a*,*d*) $\lambda = 0$, that is the uniaxial Maier–Saupe interaction potential, (*b*,*e*) $\lambda = 1/6$, (*c*,*f*) $\lambda = \lambda_{tc}^{UB} = 0.217$.

The behaviour for values of λ in the interval $(\lambda_{tc}^{(UB)}, \lambda_{tp})$ is displayed in figure 3. For values of λ in this range the model predicts two first-order phase transitions, a isotropic-to-uniaxial phase transition at high temperature (low values of t) followed by a uniaxial-to-biaxial phase transition at lower temperatures (higher values of t). While the former is associated with a shock that is static in λ, the latter is originated at the uniaxial–biaxial tricritical point and is identified by a classical shock whose location moves from low temperatures to higher temperatures as the biaxiality parameter λ increases.

As shown in figures 1 and 4*a*,*d*, for $\lambda = \lambda_{tp} = 0.234$ the system displays a triple point at which all three phases coexist. This situation is realized as the two shocks associated with the isotropic-to-uniaxial and uniaxial-to-biaxial phase transitions merge at zero external fields, giving rise to a single shock having an amplitude given by the sum of the amplitudes of the two individual shocks. Consistently with the phase diagram in figure 1, the uniaxial phase is not energetically accessible for $\lambda > \lambda_{tp}$. For instance, for $\lambda = 0.284$ (figure 4*b*,*e*), the order parameters jump from the isotropic phase to the biaxial phase as the temperature is lowered. This is also the case when $\lambda = 1/3$ (*c*,*f*). The case $\lambda = 1/3$, as also discussed in [67], leads to proportionality between the stable branches of the order parameters. Precisely this is $3m^1 \pm m^3 = 0$, corresponding to $T' = \pm S$ in the convention adopted by Virga and co-authors in [67].

For values of λ exceeding the value 1/3, the isotropic-to-biaxial phase transition remains first-order until a second tricritical point is disclosed. In figure 5, the change in order of the isotropic-to-biaxial phase transition is displayed. For $\lambda < \lambda_{tc}^{(IB)}$ (figure 5*a*,*d*) both order parameters undergo a discontinuous jump from the isotropic solution to the biaxial one. The shock disappears when $\lambda = \lambda_{tc}^{(IB)} = 2/3$ is considered (figure 5*b*,*e*), and consequently both order parameters experience a gradient catastrophe at $t = t_{tc}^{(IB)} = 3/2$. Larger values of λ lead to a direct second-order transition from the isotropic to the biaxial phase, with the transition value given by $t^{(IB)} = 1/\lambda$ (figure 5*c*,*f*).

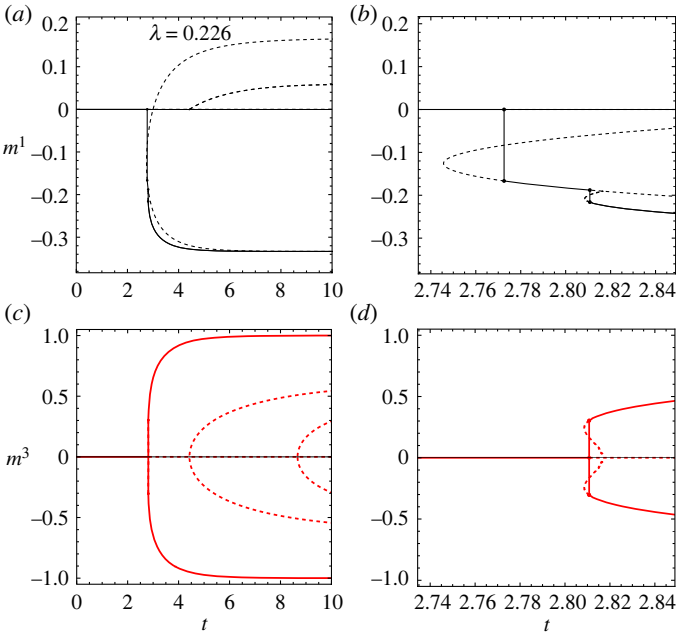

Figure 3. Order parameters in the two-parameter reduction for values of λ in the interval $\lambda_{tc}^{(UB)} \leq \lambda < \lambda_{tp}$. Panel (*a*,*c*) shows both order parameters versus t for $\lambda = 0.226 \in (\lambda_{tc}^{(UB)}, \lambda_{tp})$ as an example. Panel (*b*,*d*) displays a magnification of the order parameters around the tricritical temperature and triple point temperature.

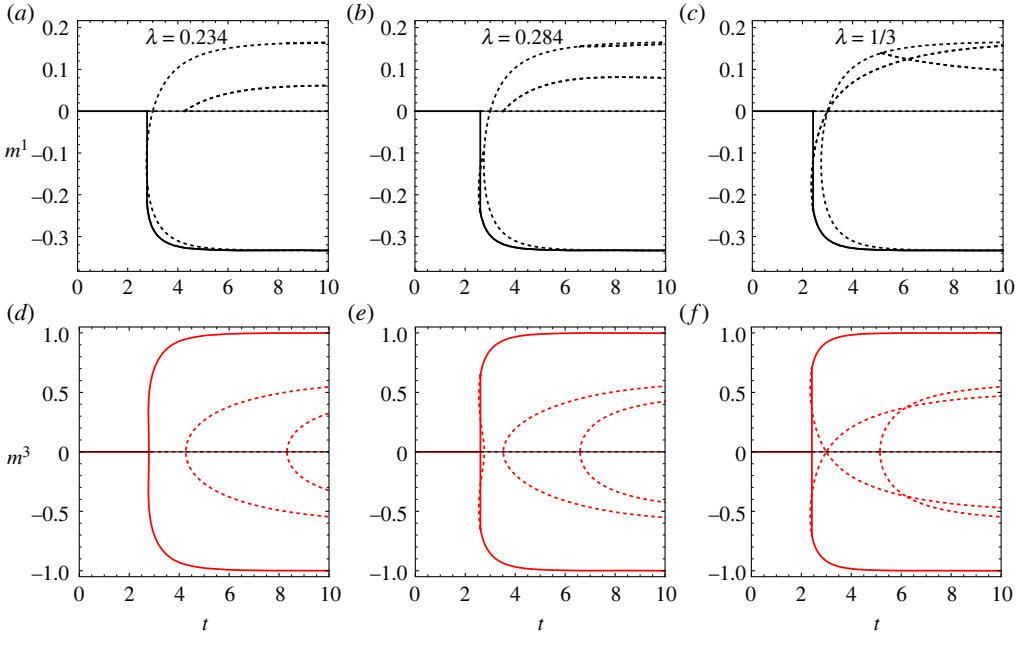

Figure 4. Order parameters in the two-parameter reduction for values of λ in the interval $\lambda_{tp} \leq \lambda \leq 1/3$. (*a*,*d*) $\lambda = \lambda_{tp} = 0.234$, (*b*,*e*) $\lambda = 0.284$, (*c*,*f*) $\lambda = 1/3$.

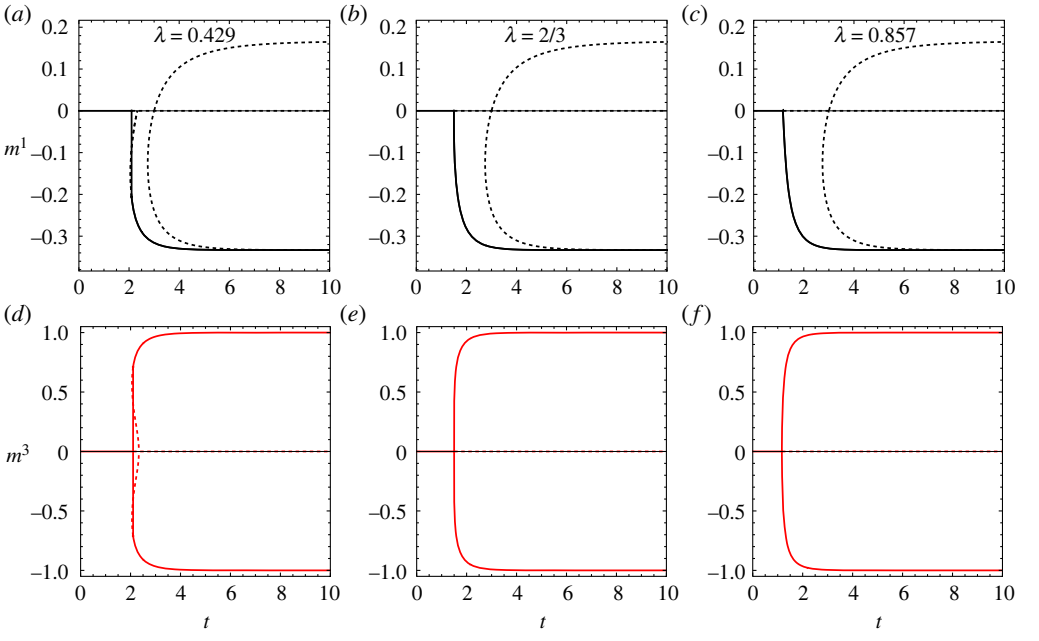

Figure 5. Order parameters in the two-parameter reduction for $\lambda > 1/3$. (*a*,*d*) $\lambda = 0.429$, (*b*,e) $\lambda = \lambda_{tc}^{(IB)} = 2/3$, (*c*,*f*) $\lambda = 0.857$.

Our results are, both qualitatively and quantitatively, consistent with previous studies [58,60,67]. In particular, according to the Monte Carlo simulation results reported in [58,60,67], the values of λ at the first and second tricritical points are approximately 0.24 and approximately 2/3, respectively. Moreover, the global Monte Carlo study performed in [60] predicts $\lambda \simeq 0.26$ for the triple point. Consistency is also shown with the extended analysis preformed in [73], where a fourth-degree Landau potential in the two tensors **Q** and **B** is considered. Indeed, the authors find a zero-fields phase diagram displaying a first- and second-order isotropic-to-uniaxial-to-biaxial phase transitions and first- and second-order isotropic-to-biaxial phase transitions, thus disclosing two tricritical points and a single triple point. On the other hand, similar but not totally equivalent phase diagram topologies are described in [14,72], where a sixth-degree Landau potential in a single-order tensor has been analysed. The phase diagram we obtain (figure 1) is also qualitatively in agreement with the one obtained in [74], where the authors derive a Landau expansion of a free energy which is intrinsically linked to a molecular-field theory, and then discuss the Sonnet–Virga–Durand limit.

It goes without saying that a single-tensor theory does not distinguish between intrinsic and phase biaxiality. This separation is made clear and sharp by starting from two molecular tensors **q** and **b** in the Hamiltonian (e.g. (2.2)) which, correspondingly, give rise macroscopically to two order tensors **Q** and **B** eventually accounting for the phase and intrinsic biaxiality, respectively. In this work, the λ-model in the absence of external fields is shown to admit two-parameter reductions, which account for isotropic, uniaxial and intrinsic biaxial phases. Other models, as for example the Maier–Saupe model (retrieved from the λ-model setting $\lambda = 0$), have been shown to produce uniaxiality and phase biaxiality at the macroscopic level and in the presence of external fields [10,95–97].

5. Concluding remarks

In this paper, we have analysed in detail a discrete mean-field model for a biaxial nematic LC subject to external fields, using an approach based on the differential identity (2.11) for the

partition function. Upon the introduction of suitable variables, namely the order parameters, the multi-dimensional linear PDE satisfied by the partition function leads, in the thermodynamic limit, to a set of equations of state involving all four orientational order parameters. The equations are completely solvable by the method of characteristics proving the integrability of the model.

Via the introduction of a novel set of order parameters corresponding to orientational Gibbs weights, we have obtained the equations of state in explicit form. We proved that, in the absence of external fields, the system is fully characterized by two-parameter reductions, and such reductions persist in the case of non-zero external fields subject to suitable constraints. A detailed analysis demonstrates the existence of a rich phase diagram, that is remarkably consistent with the results known in the literature for the standard Maier–Saupe model and its biaxial extensions. Hence, the discrete models of the type studied in this paper capture, at least qualitatively, the most important features of continuum models with external fields for which explicit analytic formulae are not available. These results indeed encourage further studies on integrable biaxial models where the Hamiltonian contains a more general nonlinear dependence on the tensors **q** and **b**, as for instance the one implied by the full Straley pair-interaction potential. Moreover, the phenomenology encoded in the equations of state (3.17*a*)–(3.17*d*) for general field values, as well as the two-parameter reductions obtained in proposition 3.5 for constrained fields, still need to be further analysed and described. Such cases are currently under investigation and results will be reported in due course.

Ethics. This work did not require ethical approval from a human subject or animal welfare committee.

Data accessibility. This article has no additional data.

Declaration of AI use. We have not used AI-assisted technologies in creating this article.

Authors' contributions. G.D.M.: conceptualization, formal analysis, funding acquisition, investigation, methodology, resources, validation, visualization, writing—original draft, writing—review and editing; F.G.: conceptualization, formal analysis, funding acquisition, investigation, methodology, resources, validation, visualization, writing—original draft, writing—review and editing; A.M.: conceptualization, formal analysis, funding acquisition, investigation, methodology, resources, validation, visualization, writing—original draft, writing—review and editing.

All authors gave final approval for publication and agreed to be held accountable for the work performed therein.

Conflict of interest declaration. We declare we have no competing interests.

Funding. A.M. is supported by the Leverhulme Trust Research Project grant no. 2017-228, the Royal Society International Exchanges grant no. IES-R2-170116 and London Mathematical Society.

Acknowledgements. We would like to thank the Isaac Newton Institute for Mathematical Sciences for the hospitality during the six-month programme 'Dispersive hydrodynamics: mathematics, simulation and experiments, with applications in nonlinear waves', Cambridge July–December 2022, under the EPSRC grant no. EP/R014604/1, where this work has been partly developed, and GNFM—Gruppo Nazionale per la Fisica Matematica, INdAM (Istituto Nazionale di Alta Matematica). F.G. also acknowledges the hospitality of the Department of Mathematics, Physics and Electrical Engineering of Northumbria University Newcastle.

References

1. Stanley HE. 1971 *Introduction to phase transitions and critical phenomena*. New York, NY: Oxford University Press, Inc.
2. Callen HB. 1985 *Thermodynamics and an introduction to thermostatistics*. Singapore: Wiley.
3. Parisi G. 1988 *Statistical field theory*. Redwood City, CA: Addison-Wesley Publishing Company.
4. Gallo I, Barra A, Contucci P. 2009 Parameter evaluation of a simple mean-field model of social interaction. *Math. Models Methods Appl. Sci.* **19**, 1427–1439. (doi:10.1142/S0218202509003863)
5. Barra A, Contucci P, Sandell R, Vernia C. 2014 An analysis of a large dataset on immigration integration in Spain: the statistical mechanics perspective of social action. *Sci. Rep.* **4**, 4174. (doi:10.1038/srep04174)
6. Agliari E, Barra A, Dello Schiavo L, Moro A. 2016, Complete integrability and information processing by biochemical reactions. *Sci. Rep.* **6**, 36314. (23p). (doi:10.1038/srep36314)

7. Agliari E, Fachechi A, Marullo C. 2022 Non-linear PDEs approach to statistical mechanics of dense associative memories. *J. Math. Phys.* **63**, 103304. (doi:10.1063/5.0095411)
8. Hopfield JJ. 1982 Neural networks and physical systems with emergent collective computational abilities. *Proc. Natl Acad. Sci. USA* **79**, 2554–2558. (doi:10.1073/pnas.79.8.2554)
9. Fedele M, Vernia C, Contucci P. 2013 Inverse problem robustness for multi-species mean-field spin models. *J. Phys. A Math. Theor.* **46**, 065001. (doi:10.1088/1751-8113/46/6/065001)
10. De Matteis G, Giglio F, Moro A. 2018 Exact equations of state for nematics. *Ann. Phys.* **396**, 386–396. (doi:10.1016/j.aop.2018.07.016)
11. Sonnet AM, Virga EG. 2012 *Dissipative ordered fluids: theories for liquid crystals*. New York, NY: Springer.
12. Zannoni C. 2022 *Liquid crystals and their computer simulations*. Cambridge, UK: Cambridge University Press.
13. Gramsbergen EF, Longa L, de Jeu WH. 1986 Landau theory of the nematic-isotropic phase transition. *Phys. Rep.* **135**, 195–257. (doi:10.1016/0370-1573(86)90007-4)
14. Mukherjee PK, Sen K. 2009 On a new topology in the phase diagram of biaxial nematic liquid crystals. *J. Chem. Phys.* **130**, 141101. (doi:10.1063/1.3117925)
15. Chillingworth DRJ. 2015 Critical points and symmetries of a free energy function for biaxial nematic liquid crystals. *Nonlinearity* **84**, 1483–1537. (doi:10.1088/0951-7715/28/5/1483)
16. Dunmur D, Sluckin T. 2011 *Soap, science, & flat-screen TVs*. Oxford, UK: Oxford University Press.
17. Freiser MJ. 1970 Ordered states of a nematic liquid. *Phys. Rev. Lett.* **24**, 1041–1043. (doi:10.1103/PhysRevLett.24.1041)
18. Yu LJ, Saupe A. 1980 Observation of a biaxial nematic phase in potassium laurate-1-decanol-water mixtures. *Phys. Rev. Lett.* **45**, 1000–1003. (doi:10.1103/PhysRevLett.45.1000)
19. Luckhurst GR. 2001 Biaxial nematic liquid crystals: fact or fiction? *Thin Solid Films* **393**, 40–52. (doi:10.1016/S0040-6090(01)01091-4)
20. Berardi R, Fava C, Zannoni C. 1995 A generalized Gay-Berne intermolecular potential for biaxial particles. *Chem. Phys. Lett.* **236**, 462–468. (doi:10.1016/0009-2614(95)00212-M)
21. Berardi R, Zannoni C. 2000 Do thermotropic biaxial nematics exist? A Monte Carlo study of biaxial Gay–Berne particles. *J. Chem. Phys.* **113**, 5971–5979. (doi:10.1063/1.1290474)
22. Praefcke K. 2001 Can thermotropic biaxial nematics be made real? *Mol. Cryst. Liq. Cryst. Sci. Technol., Sect. A* **364**, 15–24. (doi:10.1080/10587250108024977)
23. Praefcke K. 2002 Thermotropic biaxial nematics: highly desirable materials, still elusive? *Braz. J. Phys.* **32**, 564–569. (doi:10.1590/S0103-97332002000300017)
24. Görtz V, Southern C, Roberts NW, Gleeson HF, Goodby JW. 2009 Unusual properties of a bent-core liquid-crystalline fluid. *Soft Matter* **5**, 463–471. (doi:10.1039/B808283A)
25. Senyuk B, Wonderly H, Mathews M, Li Q, Shiyanovskii V, Lavrentovich OD. 2010 Surface alignment, anchoring transitions, optical properties, and topological defects in the nematic phase of thermotropic bent-core liquid crystal A131. *Phys. Rev. E* **82**, 041711. (doi:10.1103/PhysRevE.82.041711)
26. Lenmann M, Kang S, Köhn C, Haseloh S, Kolb U, Schollmeyer D, Wang Q, Kumar S. 2006 Shape-persistent V-shaped mesogens—formation of nematic phases with biaxial order. *J. Mater. Chem.* **16**, 4326–4334. (doi:10.1039/B605718G)
27. Merkel K, Kocot A, Vij JK, Korlacki R, Mehl GH, Meyer T. 2004 Thermotropic biaxial nematic phase in liquid crystalline organo-siloxane tetrapodes. *Phys. Rev. Lett.* **93**, 237801. (doi:10.1103/PhysRevLett.93.237801)
28. Figueirinhas JL, Cruz C, Filip D, Feio G, Ribeiro AC, Frère Y, Meyer T, Mehl GH. 2005 Deuterium NMR investigation of the biaxial nematic phase in an organosiloxane tetrapode. *Phys. Rev. Lett.* **94**, 107802. (doi:10.1103/PhysRevLett.94.107802)
29. Neupane K, Kang SW, Sharma S, Carney D, Meyer T, Mehl GH, Sprunt S. 2006 Dynamic light scattering study of biaxial ordering in a thermotropic liquid crystal. *Phys. Rev. Lett.* **97**, 207802. (doi:10.1103/PhysRevLett.97.207802)
30. Cordoyiannis G, Apreutesei D, Mehl GH, Glorieux C, Thoen J. 2008 High-resolution calorimetric study of a liquid crystalline organo-siloxanetetrapode with a biaxial nematic phase. *J. Phys. Rev. E* **78**, 011708. (doi:10.1103/PhysRevE.78.011708)
31. Cruz C, Figueirinhas JL, Filip D, Feio G, Ribeiro AC, Frère Y, Meyer T, Mehl GH. 2008 Biaxial nematic order and phase behavior studies in an organosiloxane

tetrapode using complementary deuterium NMR experiments. *Phys. Rev. E* **78**, 051702. (doi:10.1103/PhysRevE.78.051702)
32. Southern CD, Brimicombe PD, Siemianowski SD, Jaradat S, Roberts V, Görtz V, Goodby JW, Gleeson HF. 2008 Thermotropic biaxial nematic order parameters and phase transitions deduced by Raman scattering. *Europhys. Lett.* **82**, 56001. (doi:10.1209/0295-5075/82/56001)
33. Berardi R, Muccioli L, Orlandi S, Ricci M, Zannoni C. 2008 Computer simulations of biaxial nematics. *J. Phys.: Condens. Matter* **20**, 463101. (doi:10.1088/0953-8984/20/46/463101)
34. Tschierske C, Photinos DJ. 2010 Biaxial nematic phases. *J. Mater. Chem.* **20**, 4263–4294. (doi:10.1039/b924810b)
35. Vanakaras AG, Photinos DJ. 2008 Thermotropic biaxial nematic liquid crystals: spontaneous or field stabilized? *Chem. Phys.* **128**, 154512. (doi:10.1063/1.2897993)
36. Peroukidis SD, Karahaliou PK, Vanakaras AG, Photinos DJ. 2009 Biaxial nematics: symmetries, order domains and field-induced phase transitions. *Liq. Cryst.* **36**, 727.737 (doi:10.1080/02678290902814700)
37. Francescangeli O, Vita F, Ferrero C, Dingemans T, Samulski ET. 2011 Cybotaxis dominates the nematic phase of bent-core mesogens: a small-angle diffuse X-ray diffraction study. *Soft Matter* **7**, 895– 901. (doi:10.1039/C0SM00745E)
38. Francescangeli O, Samulski ET. 2010 Insights into the cybotactic nematic phase of bent-core molecules. *Soft Matter* **6**, 2413–2420. (doi:10.1039/c003310c)
39. Samulski ET. 2010 Meta-cybotaxis and nematic biaxiality. *Liq. Cryst.* **37**, 669–678. (doi:10.1080/02678292.2010.488938)
40. Zhang C, Sprunt S, Jákli A, Gleeson JT. 2012 Biaxial nematic order induced by smectic fluctuations. *Phys. Rev. E* **86**, 020704(R). (doi:10.1103/PhysRevE.86.020704)
41. Lehmann M. 2011 Biaxial nematics from their prediction to the materials and the vicious circle of molecular design. *Liq. Cryst.* **38**, 1389–1405. (doi:10.1080/02678292.2011.624374)
42. Karahaliou PK, Vanakaras AG, Photinos DJ. 2009 Symmetries and alignment of biaxial nematic liquid crystals. *J. Chem. Phys.* **131**, 124516. (doi:10.1063/1.3226560)
43. Gorkunov MV, Osipov MA, Kocot A, Vij JK. 2010 Molecular model of biaxial ordering in nematic liquid crystals composed of flat molecules with four mesogenic groups. *Phys. Rev. E* **81**, 061702. (doi:10.1103/PhysRevE.81.061702)
44. Osipov MA, Gorkunov MV. 2010 Ferroelectricity in low-symmetry biaxial nematic liquid crystals. *J. Phys.: Condens. Matter* **22**, 362101. (doi:10.1088/0953-8984/22/36/362101)
45. Figuerinhas JL, Feio G, Cruz C, Lehmann M, Köhn C, Dong RY. 2010 Nuclear magnetic resonance spectroscopic investigations of phase biaxiality in the nematic glass of a shape-persistent V-shaped mesogen. *J. Chem. Phys.* **133**, 174509. (doi:10.1063/1.3496491)
46. Osipov MA, Pajak G. 2012 Influence of dipole–dipole correlations on the stability of the biaxial nematic phase in the model bent-core liquid crystal. *J. Phys.: Condens. Matter* **24**, 142201. (doi:10.1088/0953-8984/24/14/142201)
47. Ghoshal N, Mukhopadhyay K, Kumar Roy S. 2012 Importance of transverse dipoles in the stability of biaxial nematic phase: a Monte Carlo study. *Liq. Cryst.* **39**, 1381–1392. (doi:10.1080/02678292.2012.717235)
48. Luckhurst GR. 2004 Liquid crystals: a missing phase found at last? *Nature* **430**, 413–414. (doi:10.1038/430413a)
49. Luckhurst GR. 2005 Thermotropic biaxial nematics: frequently asked questions. *British Liquid Crystal Society Newsletter*. 10 August. See http://blcs.eng.cam.ac.uk/wp-content/uploads/2013/05/newsletter_aug_2005.pdf.
50. Lee JH, Lim TK, Kim WT, Jin JI. 2007 Dynamics of electro-optical switching processes in surface stabilized biaxial nematic phase found in bent-core liquid crystal. *J. Appl. Phys.* **101**, 034105. (doi:10.1063/1.2433126)
51. Berardi R, Muccioli L, Zannoni C. 2008 Field response and switching times in biaxial nematics. *J. Chem. Phys.* **128**, 024905. (doi:10.1063/1.2815804)
52. Nagaraj M, Merkel K, Vij JK, Kocot A. 2010 Macroscopic biaxiality and electric-field–induced rotation of the minor director in the nematic phase of a bent-core liquid crystal. *Europhys. Lett.* **91**, 66002. (doi:10.1209/0295-5075/91/66002)
53. Pelletier O, Davidson P, Livage J. 1999 A biaxial nematic gel phase in aqueous vanadium pentoxide suspensions. *Eur. Phys. J. B* **12**, 541–546. (doi:10.1007/s100510051036)
54. van den Pol E, Petukhov AV, Thies-Weesie DME, Byelov DV, Vroege GJ. 2009 Experimental realization of biaxial liquid crystal phases in colloidal dispersions of boardlike particles. *Phys. Rev. Lett.* **103**, 258301. (doi:10.1103/PhysRevLett.103.258301)

55. van den Pol E, Thies-Weesie DME, Petukhov AV, Byelov DV, Vroege GJ. 2010 Uniaxial and biaxial liquid crystal phases in colloidal dispersions of board-like particles. *Liq. Cryst.* **37**, 641–651. (doi:10.1080/02678291003798164)
56. Mundoor H, Park S, Senyuk B, Wensink HH, Smalyukh II. 2018 Hybrid molecular-colloidal liquid crystals. *Science* **360**, 768–771. (doi:10.1126/science.aap9359)
57. Wang Z, Raistrick T, Street A, Reynolds M, Liu Y, Gleeson HF. 2022 Direct observation of biaxial nematic order in auxetic liquid crystal elastomers. *Materials* **16**, 393. (doi:10.3390/ma16010393)
58. Romano S. 2004 Computer simulation of a biaxial nematogenic model on a three-dimensional lattice and based on a recently proposed interaction potential. *Physica A* **337**, 505–519. (doi:10.1016/j.physa.2004.02.001)
59. De Matteis G, Romano S. 2008 Biaxial and uniaxial phases produced by partly repulsive mesogenic models involving D_2h molecular symmetries. *Phys. Rev. E* **78**, 021702. (doi:10.1103/PhysRevE.78.021702)
60. Sai Preeti G, Murthy KPN, Sastry VSS, Chiccoli C, Pasini P, Berardi R, Zannoni C. 2011 Does the isotropic-biaxial nematic transition always exist? A new topology for the biaxial nematic phase diagram. *Soft Matter* **7**, 11483. (doi:10.1039/c1sm06214j)
61. Bisi F, De Matteis G, Romano S. 2013 Calamitic and antinematic orientational order produced by the generalized Straley lattice model. *Phys. Rev. E* **88**, 032502. (doi:10.1103/PhysRevE.88.032502)
62. Maier W, Saupe A. 1958 Eine einfache molekulare Theorie des nematischen kristallinflüssigen Zustandes. *Z. Naturforsch. A* **13**, 564–566. (doi:10.1515/zna-1958-0716)
63. Maier W, Saupe A. 1959 Eine einfache molekular-statistische Theorie der nematischen kristallinflüssigen Phase. Teil II. *Z. Naturforsch. A* **15**, 287–292. (doi:10.1515/zna-1960-0401)
64. Straley JP. 1974 Ordered phases of a liquid of biaxial particles. *Phys. Rev. A* **10**, 1881–1887. (doi:10.1103/PhysRevA.10.1881)
65. Sonnet AM, Virga EG, Durand GE. 2003 Dielectric shape dispersion and biaxial transitions in nematic liquid crystals. *Phys. Rev. E* **67**, 061701. (doi:10.1103/PhysRevE.67.061701)
66. De Matteis G, Virga EG. 2005 Tricritical points in biaxial liquid crystal phases. *Phys. Rev. E* **71**, 061703. (doi:10.1103/PhysRevE.71.061703)
67. De Matteis G, Romano S, Virga EG. 2005 Bifurcation analysis and computer simulation of biaxial liquid crystals. *Phys. Rev. E* **72**, 041706. (doi:10.1103/PhysRevE.72.041706)
68. Bisi F, Virga EG, Gartland EC J, De Matteis G, Sonnet AM, Durand GE. 2006 Universal mean-field phase diagram for biaxial nematics obtained from a minimax principle. *Phys. Rev. E* **73**, 051709. (doi:10.1103/PhysRevE.73.051709)
69. De Matteis G, Bisi F, Virga EG. 2007 Constrained stability for biaxial nematic phases. *Contin. Mech. Thermodyn.* **19**, 1–23. (doi:10.1007/s00161-007-0041-1)
70. Romano S. 2004 Mean-field and computer simulation study of a biaxial nematogenic lattice model mimicking shape amphiphilicity. *Phys. Lett. A* **333**, 110–119. (doi:10.1016/j.physleta.2004.09.055)
71. Gartland EC, Virga EG. 2010 Minimum principle for indefinite mean-field free energies. *Arch. Ration. Mech. Anal.* **196**, 143–189. (doi:10.1007/s00205-009-0238-5)
72. Allender D, Longa L. 2008 Landau–de Gennes theory of biaxial nematics reexamined. *Phys. Rev. E* **78**, 011704. (doi:10.1103/PhysRevE.78.011704)
73. De Matteis G, Sonnet AM, Virga EG. 2008 Landau theory for biaxial nematic liquid crystals with two order parameter tensors. *Contin. Mech. Thermodyn.* **20**, 347–374. (doi:10.1007/s00161-008-0086-9)
74. Luckhurst GR, Naemura S, Sluckin TJ, Thomas KS, Turzi SS. 2012 Molecular-field-theory approach to the Landau theory of liquid crystals: uniaxial and biaxial nematics. *Phys. Rev. E* **85**, 031705. (doi:10.1103/PhysRevE.85.031705)
75. Turzi SS, Sluckin TJ. 2012 Symmetry adapted molecular-field theory for thermotropic biaxial nematic liquid crystals and its expansion at low temperature. *SIAM J. Appl. Math.* **73**, 1139–1163. (doi:10.1137/120897237)
76. To TBT, Sluckin TJ, Luckhurst GR. 2013 Biaxiality-induced magnetic field effects in bent-core nematics: molecular-field and Landau theory. *Phys. Rev. E* **88**, 062506. (13p). (doi:10.1103/PhysRevE.88.062506)
77. De Matteis G, Romano S. 2009 Mesogenic lattice models with partly antinematic interactions producing uniaxial nematic phases. *Phys. Rev. E* **80**, 031702. (doi:10.1103/PhysRevE.80.031702)

78. Bisi F, De Matteis G, Romano S. 2012 Antinematic orientational order produced by an extreme case of the generalized Straley lattice model. *Phys. Rev. E* **86**, 020702(R). (doi:10.1103/PhysRevE.86.020702)
79. Romano S, De Matteis G. 2011 Orientationally ordered phase produced by fully antinematic interactions: a simulation study. *Phys. Rev. E* **84**, 011703. (E) **84**, 059903. (doi:10.1103/PhysRevE.84.011703)
80. Zwanzig R. 1963 First-order phase transition in a gas of long thin rods. *J. Chem. Phys.* **39**, 1714–1721. (doi:10.1063/1.1734518)
81. Nascimento ES, Henriques EF, Vieira AP, Salinas SR. 2015 Maier-Saupe model for a mixture of uniaxial and biaxial molecules. *Phys. Rev. E* **92**, 062503. (10p) (doi:10.1103/PhysRevE.92.062503)
82. Brankov JG, Zagrebnov VA. 1983 On the description of the phase transition in the Husimi-Temperley model. *J. Phys. A. Math. Gen.* **16**, 2217–2224. (doi:10.1088/0305-4470/16/10/019)
83. Choquard P, Wagner J. 2004 On the 'mean field' interpretation of Burgers' equation. *J. Stat. Phys.* **116**, 843–953. (doi:10.1023/B:JOSS.0000037211.80229.04)
84. Genovese G, Barra A. 2009 A mechanical approach to meanfield spin models. *J. Math. Phys.* **50**, 053303. (doi:10.1063/1.3131687)
85. De Nittis G, Moro A. 2012 Thermodynamic phase transitions and shock singularities. *Proc. R. Soc. A* **468**, 701–719. (doi:10.1098/rspa.2011.0459)
86. Moro A. 2014 Shock dynamics of phase diagrams. *Ann. Phys.* **343**, 49–60. (doi:10.1016/j.aop.2014.01.011)
87. Barra A, Moro A. 2015 Exact solution of the van der Waals model in the critical region. *Ann. Phys.* **359**, 290–299. (doi:10.1016/j.aop.2015.04.032)
88. Giglio F, Landolfi G, Moro A. 2016 Integrable extended van der Waals model. *Physica D* **333**, 293–300. (doi:10.1016/j.physd.2016.02.010)
89. Lorenzoni P, Moro A. 2019 Exact analysis of phase transitions in mean-field Potts models. *Phys. Rev. E* **100**, 022103. (doi:10.1103/PhysRevE.100.022103)
90. Giglio F, Landolfi G, Martina L, Moro A. 2021 Symmetries and criticalities of generalised van der Waals models. *J. Phys. A: Math. Theor.* **54**, 405701. (14p). (doi:10.1088/1751-8121/ac2009)
91. Biondini G, Moro A, Prinari B, Senkevich O. 2022 *p*-star models, mean-field random networks, and the heat hierarchy. *Phys. Rev. E* **105**, 014306. (doi:10.1103/PhysRevE.105.014306)
92. Sonnet AM, Virga EG, Durand GE. 2003 Dielectric shape dispersion and biaxial transitions in nematic liquid crystals. *Phys. Rev. E* **67**, 061701. (7p). (doi:10.1103/PhysRevE.67.061701)
93. Wojtowicz PJ, Sheng P. 1974 Critical point in the magnetic field-temperature phase diagram of nematic liquid crystals. *Phys. Lett. A* **48**, 235–236. (doi:10.1016/0375-9601(74)90560-X)
94. Rosenblatt C. 1981 Magnetic field dependence of the nematic-isotropic transition temperature. *Phys. Rev. A* **24**, 2236–2238. (doi:10.1103/PhysRevA.24.2236)
95. Frisken BJ, Bergersen B, Palffy-Muhoray P. 1987 Phase behaviour of nematics in the presence of electric and magnetic fields. *Mol. Cryst. Liq. Cryst.* **148**, 45–59. (doi:10.1080/00268948708071778)
96. Dunmur DA, Palffy-Muhoray P. 1988 Effect of electric and magnetic fields on orientational disorder in liquid crystals. *J. Phys. Chem.* **92**, 1406–1419. (doi:10.1021/j100317a010)
97. Mukherjee PK, Rahman M. 2013 Isotropic to biaxial nematic phase transition in an external magnetic field. *Chem. Phys.* **423**, 178–181. (doi:10.1016/j.chemphys.2013.07.012)
98. Trojanowski K, Allender DW, Longa L, Kuúmierz LL. 2011 Theory of phase transitions of a biaxial nematogen in an external field. *Mol. Cryst. Liq. Cryst.* **540**, 59–68. (doi:10.1080/15421406.2011.568329)
99. Barra A, Di Lorenzo A, Guerra F, Moro A. 2014 On quantum and relativistic mechanical analogues in mean-field spin models. *Proc. R. Soc. A* **470**, 20140589. (doi:10.1098/rspa.2014.0589)
100. Kaiser P, Wiese W, Hess S. 1992 Stability and instability of an uniaxial alignment against biaxial distortions in the isotropic and nematic phases of liquid crystals. *J. Non-Equilib. Thermodyn.* **17**, 153. (doi:10.1515/jnet.1992.17.2.153)